



PERGAMON

International Journal of Solids and Structures 39 (2002) 4327–4362

INTERNATIONAL JOURNAL OF
SOLIDS and
STRUCTURES

www.elsevier.com/locate/ijsolstr

Electro-chemo-mechanical couplings in saturated porous media: elastic–plastic behaviour of heteroionic expansive clays

Alessandro Gajo ^a, Benjamin Loret ^{b,*}, Tomasz Hueckel ^c

^a Dipartimento di Ingegneria Meccanica e Strutturale, Università di Trento, via Mesiano 77, 38050 Trento, Italy

^b Laboratoire Sols, Solides, Structures B.P. 53X, 38041 Grenoble Cedex, France

^c Department of Civil and Environmental Engineering, Duke University, Durham, NC 27708-0287, USA

Received 6 January 2001; received in revised form 12 February 2002

Abstract

Chemically active saturated clays containing several cations are considered in a two-phase framework. The solid phase contains the negatively charged clay particles, absorbed water and ions. The fluid phase, or pore water, contains free water and ions. Electroneutrality is ensured in both phases, which gives rise to electrical fields. Water and ions can transfer between the two phases. In addition, a part of free water diffuses through the porous medium. A global understanding of all phenomena, deformation, transfer, diffusion and electroneutrality, is provided. Emphasis is laid on the electro-chemo-mechanical constitutive equations in an elastic–plastic setting. Elastic chemo-mechanical coupling is introduced through a potential, in such a way that the tangent elastic stiffness is symmetric. Material parameters needed to estimate the coupling are calibrated from specific experiments available in the recent literature. The elastic–plastic behaviour aims at reproducing qualitatively and quantitatively typical experimental phenomena observed on natural clays during chemical and mixed chemo-mechanical loadings, including chemical consolidation and swelling already described in Int. J. Solids Structures (39 (10), 2773–2806) in the simpler context of Na-Montmorillonite clays. Crucially, the successive exposure of a clay to pore solutions with chemical content dominated by a cation already present in the clay or quasi-absent leads to dramatically different volume changes, in agreement with experimental data.

© 2002 Elsevier Science Ltd. All rights reserved.

Keywords: Porous media; Elastic–plastic; Clays

1. Introduction

Swelling of clayey soils is an important factor in their engineering, but the accurate prediction of its amount and its consequences have been eluding engineers for several decades. The main reason for this is usually seen in a non-mechanical character of the phenomena involved and difficulties in linking them to

*Corresponding author.

E-mail address: benjamin.loret@inpg.fr (B. Loret).

soil mechanical analyses. Swelling is critically involved in such problems as borehole stability in petroleum extraction, liner and buffer stability in containment of nuclear or hazardous contaminants in environmental geotechnology.

In this paper, we will focus on chemically induced swelling and collapse of heteroionic clays, which constitute the majority of natural clays and a great part of engineered clays. In a preliminary paper (LHG, 2002),¹ we have addressed swelling of homoionic clays: these clays rarely occur in natural conditions, but they can be manufactured for specific industrial applications. Homoionic clays serve also as a good material model for some preliminary studies.

The microstructure, and especially the organization of water in different pore spaces, is very much the same in both homoionic and heteroionic clays; it has been described in detail in LHG (2002). In both cases, swelling arises as a result of chemical or electrochemical disequilibrium of a structural unit comprising:

- an amorphous substructure of quasi-crystals (clusters) of the parallel clay mineral platelets,
- absorbed water within the quasi-crystals and adsorbed water enveloping the substructure,
- the free pore water, and critically,
- ions in the interplatelet space and in the free water.

Chemical swelling here will cover both *crystalline swelling* due to absorption of water into interlamellar space and *osmotic swelling* due to adsorption of water to the external surface, and no distinction will be made between adsorbed and absorbed water. The amorphous structure is conceptualized as being wrapped in a semi-permeable membrane. This membrane serves as a gate-keeper for ion and water transfer between the free pore water and the clusters including the absorbed water. Unlike in biological tissues, such a membrane is not a physical object, rather it is a separation across which the two types of water fractions exchange cations at a certain rate.

1.1. Previous mechanical approaches

The approach to modeling of the mechanical aspects of clay swelling usually depends on the application in hand and specific processes involved.

In petroleum engineering, stability of the wellbore can be improved by circulating a mud that creates an osmotic membrane impermeable, at least partially depending on the chemical composition of the mud, to salts: if p_m , p_r are the pressures and x_m , x_r the salt molar fractions of the mud applied to the wellbore and of the rock respectively, water flow will cease when the chemical potentials equilibrate, which implies the differences $p_m - p_r$ and $x_m - x_r$ to be of the same sign.

For a sufficient difference in salinity, the pore pressure in the rock at equilibrium may be forced to be smaller than its initial value, Charlez et al. (1998). Simulations of this phenomenon have been presented by Sherwood (1994a,b), using a constitutive behaviour referred to as *inert*, Sherwood (1993). The problem of hydration and dehydration of rocks has been addressed by Heidug and Wong (1996). However, the above works do not treat separately transport and transfer phenomena, that is, they do not recognize that the changes of mass are due to both a transfer (or reactive) contribution and a diffusive contribution. This distinction is necessary to provide elastic constitutive equations that describe coupling effects in swelling clays, and it will be stressed in the present formulation.

Ma and Hueckel (1992), Hueckel (1992a,b) proposed to treat clays exposed to thermal and chemical loads as a two phase mixture, with absorbed water being a part of solid phase, and an inter-phase transfer to model its absorption and desorption process. Bennethum and Cushman (1999) and Murad (1999) have

¹ LHG (2002) is an abbreviation for Loret et al. (2002).

addressed the transfer of water into interlamellar space in clays through a two- or three-spatial scale modeling using homogenization schemes. This type of approach entails a substantial number of constitutive assumptions, requiring sophisticated identification procedures. A multi-constituent mixture, involving charged species and thermal effects, has been suggested by Huyghe and Janssen (1999), but this general framework does not account for the special configuration of clays that will be developed in this work.

1.2. A model for electro-chemo-mechanical couplings

The model developed here to account for the electrical and chemical interactions with the mechanical behaviour of clays capitalizes upon a previous analysis described in LHG (2002) where electrical effects were disregarded.

Saturated clay is considered as a porous deformable continuum consisting of two overlapping phases, each phase containing several species. A kinematic criterion is used for phase identification and the absorbed water is attributed to the solid phase based on the affinity of their velocities. Capital in the modeling of deformable porous media is the coupling of the deformation of pore space in soil and the concomitant in- or out-flow of pore liquid. In chemically sensitive soils, this coupling is additionally affected by the presence of charged species in both phases. Thus, mechanics of the medium, e.g. balance of momentum, is considered at the phase level, whereas chemical processes, i.e. balances of masses, concern the species. The link between the two levels is obtained through energetic considerations. Whether or not the electro-chemical potentials are in equilibrium, water absorbed between the clay platelets can transfer into free pore water, or conversely, depending on the chemical composition of the clay and pore water phases, and on the mechanical conditions in terms of volume and pressure (Fig. 1).

The electro-chemo-mechanical elastic–plastic constitutive equations involve the species of the solid phase (the clay platelets) but treat the fluid phase as a whole. The species of the latter only diffuse through the porous medium, obeying generalized Darcy's diffusion equations. The transfer of absorbed water and species between the solid and fluid phases involves a fictitious membrane surrounding the clay platelets, which may be permeable to the chemical species at various degrees. For the sake of simplicity, all chemical species that appear in the present analysis, except clay particles, can cross the membrane. Electroneutrality is required in each of the two phases, giving rise to an electrical field.

The theoretical framework is illustrated by simulations of typical phenomena observed during laboratory experiments: the change of chemical composition of pore water has, due to the electro-chemo-mechanical couplings, consequences on the mechanical state of the porous medium. Parameters involved in the model are calibrated. Mechanical, chemical and chemo-mechanical loading and unloading paths are considered. The basic behaviour described for neutral species in LHG (2002) still holds for purely mechanical loadings. On the other hand, substantial differences appear for chemical loadings and unloadings. Increase of the salinity of pore water at constant confinement leads to a volume decrease, so-called *chemical consolidation*. Subsequent exposure to a distilled water solution displays *swelling*. For pure Na-Montmorillonite clays, however, the latter is smaller than the chemical consolidation so that the chemical loading cycle results in a net contractancy whose amounts increases with the confinement. The situation is quite different here as the influence of ionic species on mechanical properties vary greatly from one species to the other. Replacement of a Na-dominated pore solution by distilled pore water produces a quite different swelling strain than if the replacement were made using a K-dominated pore solution, Di Maio and Fenelli (1997). Of course, the details of the initial ionic content of the clay clusters is of capital importance in these processes.

With respect to previous publications, the key feature of the present analysis is that the constitutive model developed is more than qualitative. It embodies not only elasticity but also elasto-plasticity which is a necessary requirement to simulate the key features of the chemo-mechanical behaviour of swelling clays, as highlighted by experimental data which have been recently published. On the other hand, as a first

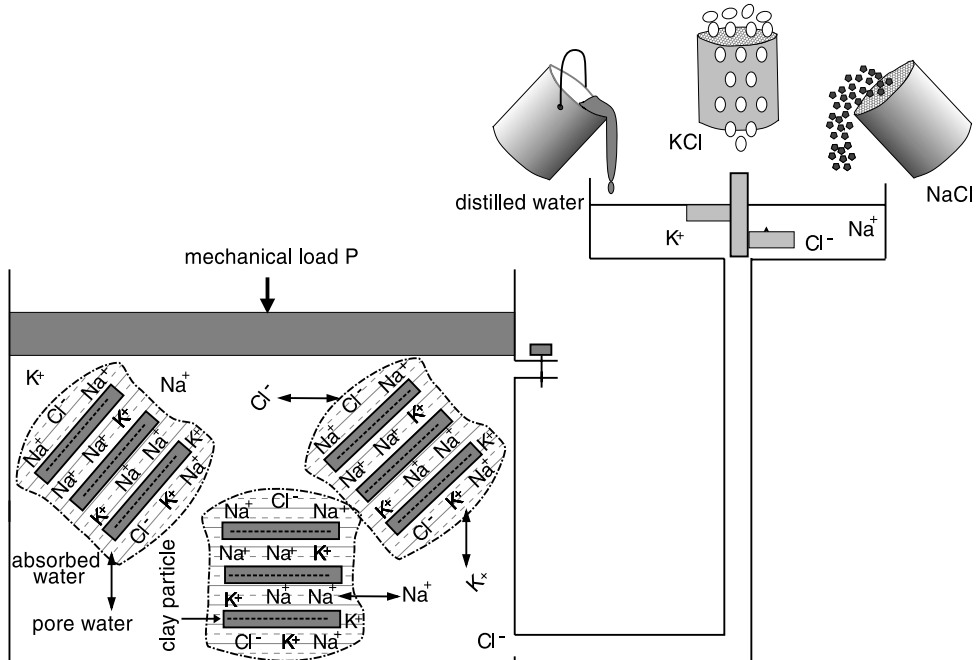


Fig. 1. Schematic of a chemo-mechanical experiment. The pore water is in contact with a large recipient whose chemical composition is controlled. In the sample submitted to a variable mechanical load in terms of stress or strain, schematized here by P , the solid phase (clay clusters with absorbed water and ions) is in contact with the fluid phase (pore water). Water and ions absorbed in the solid phase are exchanged with their counterparts in pore water depending on their respective contents and on mechanical conditions.

attempt, only two cations are assumed to be present in the clay clusters. While natural clays contain certainly more cations, their relative influence on the mechanical response of the clays certainly depends on the electrolyte filling the pore space. Therefore, extension of the model to clays with many ionic species requires experimental data to be available.

Although attention is paid mainly to the elastic–plastic constitutive equations, the latter are shown to be embedded in a general formulation where both transfer and diffusion processes can be considered in initial and boundary value problems to be treated through the finite element method in a work under development, Gajo and Loret (2002).

Notation: Compact or index tensorial notation will be used throughout this work. Tensor quantities are identified by boldface letters. $\mathbf{I} = (I_{ij})$ is the second order identity tensor (Kronecker delta). Symbols ‘ \cdot ’ and ‘ $\cdot\cdot$ ’ between tensors of various orders denote their inner product with single and double contraction respectively. tr denotes the trace of a second order tensor, dev its deviatoric part and div is the divergence operator.

2. The two-phase framework

2.1. General framework

We consider a two-phase porous medium. Each phase is composed of several species:

- the *solid phase* S contains five species

$$\left\{ \begin{array}{l} \text{clay particles} \\ \text{absorbed and adsorbed water} \\ \text{ions sodium, potassium, chloride} \end{array} \right. \quad \begin{array}{l} \text{denoted by the symbol} \\ \text{c} \\ \text{w} \\ \text{Na}^+, \text{K}^+, \text{Cl}^- \end{array} \quad (2.1)$$

- the *fluid phase* W contains four species

$$\left\{ \begin{array}{l} \text{pore water} \\ \text{ions sodium, potassium, chloride} \end{array} \right. \quad \begin{array}{l} \text{denoted by the symbol} \\ \text{w} \\ \text{Na}^+, \text{K}^+, \text{Cl}^- \end{array} \quad (2.2)$$

The clay clusters are surrounded by a fictitious membrane which is a priori impermeable to clay particles only: the mass of clay in the solid phase, obtained by aggregation of clay clusters, is constant,

$$m_{cS} = \text{constant}. \quad (2.3)$$

However, the membrane could serve also as a barrier for anions or non-exchangeable cations. As a rule, a species in a phase is referred by two indices, the index of the species and the index of the phase. We shall introduce several sets of species with specific properties, namely:

- species in the solid phase $S = \{w, \text{Na}^+, \text{K}^+, \text{Cl}^-, c\}$;
- species in the fluid phase $W = \{w, \text{Na}^+, \text{K}^+, \text{Cl}^-\}$;
- species that can cross the membrane, $S^{\leftrightarrow} = W^{\leftrightarrow} = W = \{w, \text{Na}^+, \text{K}^+, \text{Cl}^-\}$;
- cations in the solid phase $S^+ = \{\text{Na}^+, \text{K}^+\}$.

The main assumptions which underly the two-phase model follow the *strongly interacting* model of Bataille and Kestin (1977), namely,

- (H1) For each species, only the mass balance is required, but not the momentum balance;
- (H2) Mass balance for each phase is obtained via mass balances of the species it contains. Momentum balances are required for each phase.
- (H3) The velocity of any species in the solid phase is that of the latter, $\mathbf{v}_{kS} = \mathbf{v}_S, \forall k \in S$.
- (H4) In the fluid phase, pressure is assumed to be uniform across all species, $p_{kW} = p_W, \forall k \in W$, but each species k is a priori endowed with its own velocity \mathbf{v}_{kW} .
- (H5) Electroneutrality is required in both phases. In the solid phase, negatively charged clay particles require the presence of the cations.

In the solid phase, the pressures attributed to the phase and to the species in that phase are not set a priori as equal. This is motivated by the role that absorbed water, which is one of the solid phase species, may have in transmitting a part of the total stress.

2.2. Basic entities

The incremental work done by the total stress $\boldsymbol{\sigma}$ in the incremental strain $\delta\boldsymbol{\epsilon}$ of the solid phase and by the *electro-chemical potentials* μ_{kk}^{ec} during the addition/subtraction of mass δm_{kk} to/from the species k of the phase K is

$$\delta\Psi = \boldsymbol{\sigma} : \delta\boldsymbol{\epsilon} + \sum_{k,K} \mu_{kk}^{\text{ec}} \delta m_{kk}. \quad (2.4)$$

Summation extends to all $k \in S^{\leftrightarrow} = W^{\leftrightarrow} = W$ and $K = S, W$, since the contribution due to the clay particles vanishes due to (2.3). The electro-chemical potentials [unit: m^2/s^2] are mass-based and the m_{kk} 's are the

fluid-mass contents per unit initial volume of the porous medium [unit: kg/m³]. Since the volume of the solid phase is also the volume of the porous medium, $\text{tr } \epsilon$ is the relative volume change of both these quantities.

Another convention is to measure the amount of species by the number of moles per initial volume and to use mole-based (electro-)chemical potentials,

$$g_{kk}^{(\text{ec})} = m_k^{(\text{M})} \mu_{kk}^{(\text{ec})}, \quad (2.5)$$

with $m_k^{(\text{M})}$ molar mass of species k , e.g. $m_w^{(\text{M})} = 18$ g. The constitutive equations will be phrased in terms of mass-based (electro-)chemical potentials, with the mass-contents as independent variables. However, data are available for mole-based free enthalpies of formation. Therefore, use will be made of the entities best appropriate to the context.

The classic formula of the chemical potential g_{kw} of the species k in the fluid phase W , e.g. Haase (1990, Chapter 2–5); Kestin (1968, Chapter 21), identifies a purely mechanical contribution which involves

- the *intrinsic pressure* of the fluid phase p_w ,
- the *molar volume of the species* $v_{kw}^{(\text{M})}$,

and a chemical contribution which accounts for the *molar fraction* x_{kw} of the species k in phase W . For charged species in presence of the electrical field ϕ^W , the electro-chemical potential g_{kw}^{ec} involves in addition an electrical contribution. Soluble species develop also a configurational energetic property measured by their free enthalpy of formation g_{kw}^0 . In integral form,

$$g_{kw}^{\text{ec}} = m_k^{(\text{M})} \mu_{kw}^{\text{ec}} = g_{kw}^0 + \int v_{kw}^{(\text{M})} \, \text{d}p'_w + RT \ln x_{kw} + \zeta_k \mathcal{F} \phi^W, \quad k \in W. \quad (2.6)$$

The integration above is performed from a reference state, say $(p_w = p_w^0, x_{kw} = 1, \phi^W = 0)$, to the current state. Therefore, g_{kw}^0 serves as the mole-based value of the chemical potential in the reference state. As for the species within the solid phase S , the mechanical contribution to the electro-chemical potential of species k involves its intrinsic mean-stress p_{ks} ,

$$g_{ks}^{\text{ec}} = m_k^{(\text{M})} \mu_{ks}^{\text{ec}} = g_{ks}^0 + \int v_{ks}^{(\text{M})} \, \text{d}p'_{ks} + RT \ln x_{ks} + \zeta_k \mathcal{F} \phi^S, \quad k \in S. \quad (2.7)$$

In these formulas, $R = 8.31451$ J/mol/°K is the universal gas constant, and T (°K) the absolute temperature. The electrical contribution to the mass-based chemical potentials will be introduced through the constant ζ_k that involves, besides the molar mass $m_k^{(\text{M})}$, the valence ζ_k and Faraday's equivalent charge $\mathcal{F} = 96,487$ C/mol,

$$\zeta_k = \frac{\zeta_k \mathcal{F}}{m_k^{(\text{M})}}, \quad k \in W, S. \quad (2.8)$$

By convention, $\zeta_w = 0$, and so $\zeta_w = 0$.

The density of absorbed water is reported to be non-uniform between the platelets and to be slightly higher than that of free water. However, some algebraic simplifications arise if we assume the density of any species to be one and the same in both solid and fluid phases,

$$\rho_{ks} = \rho_{kw}, \quad k \in S^{\leftrightarrow} = W^{\leftrightarrow}. \quad (2.9)$$

One of the principal tasks in building a theory of deformable porous media is to link the change of pore space to the mass of pore liquid flowing in or out of the representative volume element. This description is more complex when reactions take place, resulting in generation or disappearance of mass of some species. We shall define below different measures of mass changes and volume changes that will be used in the constitutive equations.

The *molar fraction* x_{kK} of the species k in phase K is defined by the relative ratio of the mole number N_{kK} of that species within the phase K , namely

$$x_{kK} = \frac{N_{kK}}{\sum_{l \in K} N_{lK}}. \quad (2.10)$$

Summation extends to all species in the phase K . By their definition, the molar fractions satisfy the closure relation

$$\sum_{k \in K} x_{kK} = 1, \quad K = S, W. \quad (2.11)$$

Let the initial volume of the porous medium be V_0 and let $V = V(t)$ be its current volume. The current volume of the species k of phase K is denoted by V_{kK} and the current volume of phase K by V_K . Then the *volume fraction* of the species k of phase K is defined as

$$n_{kK} = \frac{V_{kK}}{V}, \quad (2.12)$$

while the volume fraction of phase K is

$$n_K = \frac{V_K}{V} = \sum_{k \in K} n_{kK} \quad \text{with} \quad n_S + n_W = 1. \quad (2.13)$$

On the other hand, *volume contents* v_{kK} for the species k of phase K and v_K for the phase K refer to the initial total volume V_0 , namely,

$$v_{kK} = \frac{V_{kK}}{V_0} = n_{kK} \frac{V}{V_0}, \quad v_K = \frac{V_K}{V_0} = n_K \frac{V}{V_0}. \quad (2.14)$$

The *mass contents* m_{kK} per unit initial volume V_0 of the species k of phase K , and m_K of the phase K , are obtained from the volume contents v_{kK} and *intrinsic* mass densities ρ_{kK} :

$$m_{kK} = \frac{M_{kK}}{V_0} = \frac{N_{kK} m_k^{(M)}}{V_0} = \rho_{kK} v_{kK} \quad (\text{no summation on } k, K), \quad m_K = \frac{M_K}{V_0} = \sum_{k \in K} m_{kK}. \quad (2.15)$$

The *apparent* density of the species k in the porous medium, namely ρ^{kK} , and the *apparent* density of the phase K , namely ρ^K , are,

$$\rho^{kK} = n_{kK} \rho_{kK} \quad (\text{no summation on } k, K), \quad \rho^K = \sum_{k \in K} \rho^{kK}. \quad (2.16)$$

With (2.15), the molar fractions x_{kK} can be expressed in terms of the mass-contents

$$x_{kK} = \frac{m_{kK}/m_k^{(M)}}{\sum_{l \in K} m_{lK}/m_l^{(M)}}. \quad (2.17)$$

For the record, let us note the partial derivative,

$$\frac{\partial x_{kK}}{\partial m_{lK}} = \frac{x_{lK}}{m_{lK}} (I_{kl} - x_{kK}), \quad \forall k, l \in K. \quad (2.18)$$

The molar volume $v_{kK}^{(M)}$ and molar mass $m_k^{(M)}$ of the species k of phase K are linked by the intrinsic density ρ_{kK} ,

$$m_k^{(M)} = \rho_{kK} v_{kK}^{(M)} \quad (\text{no summation on } k, K), \quad (2.19)$$

so that, in incremental form, the mechanical contribution to the mass-based potential is $\delta p_W/\rho_{kW}$ for the species k of the fluid phase and $\delta p_{kS}/\rho_{kS}$ for the species k of the solid phase. Note that, if the densities are assumed to be independent of the phases, Eq. (2.9), so do the molar volumes. The *molar volume* of the fluid phase is

$$v_W^{(M)} = \sum_{k \in W} x_{kW} v_{kW}^{(M)}. \quad (2.20)$$

We will also need the concentrations which are the densities referred to the fluid phase rather than to the porous medium, namely

$$c_{kW} = \frac{\text{mass of species } k \text{ of fluid phase}}{\text{volume of fluid phase}} = \frac{M_{kW}}{V_W} = \frac{\rho^{kW}}{n_W} = \frac{m_{kW}}{v_W}, \quad k \in W. \quad (2.21)$$

From (2.20) and (2.21) follows

$$c_{kW} = \frac{m_k^{(M)} N_{kW}}{v_W^{(M)} \sum_{l \in W} N_{lW}} = \frac{m_k^{(M)}}{v_W^{(M)}} x_{kW}, \quad k \in W \quad (\text{no summation on } k). \quad (2.22)$$

An additional phase entity of physical importance in electrolytes is the electrical density: in phase K , I_{eK} is defined as

$$I_{eK} = \frac{\mathcal{F}}{V} \sum_{k \in K} \zeta_k N_{kK} = \frac{V_0}{V} \sum_{k \in K} \zeta_k m_{kK}. \quad (2.23)$$

The last equality is due to the definition (2.8) and to the definition (2.15). The fulfillment of *electroneutrality* in phase K can be expressed in various forms, e.g.

$$I_{eK} = 0 \iff \sum_{k \in K} \zeta_k x_{kK} = 0 \iff \sum_{k \in K} \zeta_k N_{kK} = 0. \quad (2.24)$$

The electroneutrality condition restricts the minimal admissible values of the molar fractions of the absorbed cations, especially when the pore solution is distilled water. Then at equilibrium, the molar fraction of absorbed water overweights the other molar fractions. However, electroneutrality implies

$$\zeta_{\text{Na}} x_{\text{NaS}} + \zeta_{\text{K}} x_{\text{KS}} = X \equiv -\zeta_{\text{C}} x_{\text{CS}} - \zeta_{\text{Cl}} x_{\text{CLS}} > 0. \quad (2.25)$$

Therefore, in the plane $(x_{\text{NaS}}, x_{\text{KS}})$, the triangle defined by the points $(0,0)$, $(X/\zeta_{\text{Na}}, 0)$ and $(0, X/\zeta_{\text{K}})$ is inaccessible, see Fig. 2.

2.3. The Gibbs–Duhem relation

For a fluid phase, the Gibbs–Duhem relation provides the fluid pressure p_W in terms of the chemical potentials of the species μ_{kW} , namely Haase (1990, Chapter 1–13). Using (2.22), the pressure is expressed in terms of the electro-chemical potentials as,

$$\delta p_W = \sum_{k \in W} c_{kW} \delta \mu_{kW}^{\text{ec}} - \frac{I_{eW}}{n_W} \delta \phi^W. \quad (2.26)$$

This relation is easy to retrieve from the definitions above by forming a linear combination of the chemical potentials (2.6) that eliminates the chemical contribution via (2.11); the result follows by using successively (2.19), (2.20) and (2.22). The last term in (2.26) is kept for the sake of generality but it vanishes for an electrically neutral fluid phase, Eq. (2.24).

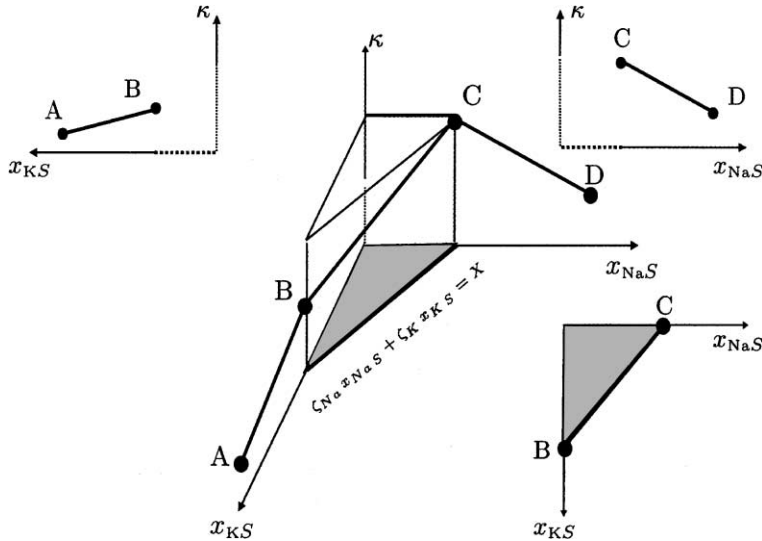


Fig. 2. Due to electroneutrality, the molar fractions of the cations are excluded from a triangular zone adjacent to the origin, Eq. (2.25). Some material properties, like the elastic compliance κ , are interpolated from the molar fractions of the cations, taking the Na-plane, i.e. $x_{\text{Ks}} = 0$, and K-plane, i.e. $x_{\text{NaS}} = 0$, as references.

In order to define the mechanical constitutive equations of the porous medium, we will need to isolate the electro-chemical effects in pore water. For that purpose, following Heidug and Wong (1996), we define the electro-chemical energy per current unit volume of the fluid phase through its differential

$$\delta\psi_W = \sum_{k \in W} \mu_{kW}^{\text{ec}} \delta c_{kW} - \delta \left(\frac{I_{\text{e}W}}{n_W} \right) \phi^W, \quad (2.27)$$

which, via the Gibbs–Duhem relation (2.26), can be integrated, up to a constant, to yield

$$\psi_w = \sum_{k \in W} \mu_{kw}^{\text{cc}} c_{kw} - \frac{I_{\text{e}w}}{n_w} \phi^w - p_w. \quad (2.28)$$

Thus, the electro-chemical energy of the fluid phase per unit initial volume of porous medium is, using (2.21),

$$\Psi_W = \psi_W \frac{V_W}{V_0} = \psi_W v_W = \sum_{k \in W} \mu_{kW}^{\text{ec}} m_{kW} - \frac{V}{V_0} I_{\text{e}W} \phi^W - p_W v_W. \quad (2.29)$$

Due to the Gibbs–Duhem relation (2.26), the differential $\delta\Psi_W$ simplifies to

$$\delta\Psi_W = \sum_{k \in W} \mu_{kW}^{\text{ec}} \delta m_{kW} - \phi^W \sum_{k \in W} \xi_k \delta m_{kW} - p_W \delta v_W. \quad (2.30)$$

Let us reiterate that the coefficients of ϕ^W in (2.26)–(2.30) vanish when electroneutrality (2.24) is required in the fluid phase.

2.4. Incompressibility constraint

A situation of particular interest arises when all species are incompressible,

$$\delta\rho_{kk} = 0, \quad \forall k, K. \quad (2.31)$$

Then, there exists a relation between the set of variables $\{\epsilon, v_W, \{m_{kS}, k \in S^\leftrightarrow\}\}$. Due to a simple extension of a result in Appendix A of LHG (2002), the increment of fluid volume content can be expressed as,

$$\delta v_W = \delta \text{tr} \epsilon - \sum_{k \in S^\leftrightarrow} \frac{\delta m_{kS}}{\rho_{kS}}. \quad (2.32)$$

3. Elastic constitutive equations

The absorption and desorption of water and ionic species to/from the solid phase introduce electro-chemo-mechanical couplings. On the other hand, the mere presence of ions in the water phase does not affect directly the mechanical behaviour of the porous medium, they just flow through. Their amount is governed by an equation of mass conservation and a flow equation. Therefore, to develop the electro-chemo-mechanical constitutive equations, we will treat the fluid phase as a whole and, temporarily ignore its chemical composition. Thus constitutive equations are provided for the following variables:

- a stress–strain couple attached to the mechanical state of the solid phase, namely (σ, ϵ) ;
- a pressure–volume couple attached to the mechanical state of the fluid phase, namely (p_W, v_W) ;
- as many couples of (electro-)chemical potential–mass content as there are species that can cross the membrane, namely $(\mu_{kS}^{(ec)}, m_{kS}), k \in S^\leftrightarrow$.

Incompressibility of the species reduces the number of unknowns and equations by one. The electrical field difference $\phi^S - \phi^W$ appears as a Lagrangian associated to the constraint represented by the electro-neutrality condition; one may pose formally $\phi^W = 0$ and then $\mu_{kW}^{ec} = \mu_{kW}, \forall k \in W$.

3.1. The global picture: deformation, mass transfer, diffusion and electroneutrality

The change of mass of each species is a priori due to both *mass transfer*, i.e. physico-chemical reaction, and *diffusion*, namely

$$\frac{\delta m_{kK}}{\delta t} = \frac{\delta}{\delta t} m_{kK}^{\text{reactive}} + \frac{\delta}{\delta t} m_{kK}^{\text{diffusive}}. \quad (3.1)$$

In practice, the changes in the species of the solid phase are purely reactive, namely by transfer, through the membrane, of water and ions between the solid and fluid phases. On the other hand, the species of the fluid phase may also undergo mass changes by transport (diffusion) from/to the outside of the representative elementary volume, i.e.

$$\frac{\delta}{\delta t} m_{kK}^{\text{diffusive}} = -\text{div} \mathbf{M}_{kK}, \quad (3.2)$$

where \mathbf{M}_{kK} is the mass flux of the species k of phase K through the solid, namely,

$$\mathbf{M}_{kK} = \rho^{kK} (\mathbf{v}_{kK} - \mathbf{v}_S). \quad (3.3)$$

Due to assumption (H3), only the fluxes of species of the fluid phase are non-zero. $\delta m_{kK}^{\text{reactive}} / \delta t$, abbreviated to $\hat{\rho}^{kK}$ in the sequel, is the *rate of transfer* of mass density towards the species k of phase K . Since this transfer concerns a single species, then

$$\hat{\rho}^{kS} + \hat{\rho}^{kW} = 0, \quad \forall k \in S^\leftrightarrow = W^\leftrightarrow. \quad (3.4)$$

In the absence of thermal effects, starting from the statements of balance of mass for each species, and of momentum and energy for the phases, e.g. Eringen and Ingram (1965), the Clausius–Duhem inequality for a mixture as a whole can be cast in the following form,

$$\delta D = -\delta\Psi + \boldsymbol{\sigma} : \delta\boldsymbol{\epsilon} - \sum_{k,K} \operatorname{div}(\mu_{kk}^{\text{ec}} \mathbf{M}_{kk}) \delta t \geq 0. \quad (3.5)$$

Using (3.1), (3.2), δD may advantageously be rewritten in a form that highlights mechanical, transfer and diffusion contributions, namely,

$$\delta D = -\delta\Psi + \boldsymbol{\sigma} : \delta\boldsymbol{\epsilon} + \sum_{k,K} \mu_{kk}^{\text{ec}} (\delta m_{kk} - \hat{\rho}^{kk} \delta t) - \sum_{k,K} \nabla \mu_{kk}^{\text{ec}} \cdot \mathbf{M}_{kk} \delta t \geq 0. \quad (3.6)$$

Consequently, the Clausius–Duhem inequality can be viewed as the sum of three contributions $\delta D = \delta D_1 + \delta D_2 + \delta D_3$, of work, mass transfer and diffusion, which will be required to be positive individually,

$$\begin{cases} \delta D_1 = -\delta\Psi + \boldsymbol{\sigma} : \delta\boldsymbol{\epsilon} + \sum_{k,K} \mu_{kk}^{\text{ec}} \delta m_{kk} \geq 0, \\ \delta D_2 / \delta t = -\sum_{k \in S^\leftrightarrow} (\mu_{ks}^{\text{ec}} - \mu_{kW}^{\text{ec}}) \hat{\rho}^{ks} \geq 0, \\ \delta D_3 / \delta t = -\sum_{k \in W} \nabla \mu_{kW}^{\text{ec}} \cdot \mathbf{M}_{kW} \geq 0. \end{cases} \quad (3.7)$$

The chemo-hyperelastic behaviour will be constructed in order for the first term δD_1 to exactly vanish. Observe that, due to electroneutrality, the electrical field does not work. Then the electro-chemical potentials in δD_1 can be replaced by the chemical potentials:

$$\delta D_1 = -\delta\Psi + \boldsymbol{\sigma} : \delta\boldsymbol{\epsilon} + \sum_{k,K} \mu_{kk} \delta m_{kk} \geq 0. \quad (3.8)$$

Consequently, the constitutive relations do not depend directly on the electrical field. Satisfaction of the second and third inequalities motivates generalized transfer equations and generalized diffusion equations respectively, as detailed in Gajo and Loret (2002). Transfer equations can readily be read off δD_2 while diffusion equations require some rewriting of δD_3 that highlights specific conjugate flux-force couples. If not neglected, body force and acceleration terms would appear in δD_3 .

3.2. Dependent and independent variables

In view of extension to the elastic–plastic behaviour, generalized strains will henceforth be denoted by a superscript el. Instances are strains, volume and mass contents, number of moles. Later, these entities will be decomposed into an elastic, or reversible, part and a plastic, or irreversible, part. Given a reference state, and a process which is reversible from that reference state to the current state, the elastic, or reversible, part of each of above entities is by convention equal to the total entity.

When the behaviour is elastic, the energy per unit initial volume of porous medium $\mathcal{W}^{\text{el}} = \Psi^{\text{el}} - \Psi_W^{\text{el}}$ can be viewed as the elastic energy of the porous medium for which the electro-chemical effects in the fluid phase are disregarded. It depends on the restricted set of independent variables ² $\{\boldsymbol{\epsilon}^{\text{el}}, v_W^{\text{el}}, \{m_{ks}^{\text{el}}, k \in S^\leftrightarrow\}\}$; indeed, with the work definition (2.4) and (2.30) and accounting for electroneutrality, its differential simplifies to

$$\delta\mathcal{W}^{\text{el}} = \boldsymbol{\sigma} : \delta\boldsymbol{\epsilon}^{\text{el}} + p_W \delta v_W^{\text{el}} + \sum_{k \in S^\leftrightarrow} \mu_{ks} \delta m_{ks}^{\text{el}}. \quad (3.9)$$

From this total differential emerge constitutive equations for the dependent variables $\{\boldsymbol{\sigma}, p_W, \{\mu_{ks}, k \in S^\leftrightarrow\}\}$ in terms of the independent variables $\{\boldsymbol{\epsilon}^{\text{el}}, v_W^{\text{el}}, \{m_{ks}^{\text{el}}, k \in S^\leftrightarrow\}\}$ in the following format

² Notice that only the arguments that vary during loadings are listed; for example, since the mass of clay is constant inside the solid phase, its influence is not shown explicitly in the list of arguments although it is tacitly assumed; this is why the superscript el is used on top of the above energies.

$$\boldsymbol{\sigma} = \frac{\partial \mathcal{W}^{\text{el}}}{\partial \boldsymbol{\epsilon}^{\text{el}}}, \quad p_W = \frac{\partial \mathcal{W}^{\text{el}}}{\partial v_W^{\text{el}}}, \quad \mu_{kS} = \frac{\partial \mathcal{W}^{\text{el}}}{\partial m_{kS}^{\text{el}}}, \quad k \in S^{\leftrightarrow}. \quad (3.10)$$

Alternative choices in the sets of independent and dependent variables can be postulated by partial or total Legendre transforms of \mathcal{W}^{el} .

3.3. Incompressible species

The formulation is simplified when all species are incompressible. We shall adopt $\{\boldsymbol{\epsilon}^{\text{el}}, \{m_{kS}^{\text{el}}, k \in S^{\leftrightarrow}\}\}$ as independent variables and then the increment of elastic fluid volume content is given by (2.32), since we require the incompressibility condition to hold in both the elastic and elastic–plastic regimes. Hence, $\delta\mathcal{W}^{\text{el}}$, Eq. (3.9), becomes

$$\delta\mathcal{W}^{\text{el}} = \bar{\boldsymbol{\sigma}} : \delta\boldsymbol{\epsilon}^{\text{el}} + \sum_{k \in S^{\leftrightarrow}} \bar{\mu}_{kS} \delta m_{kS}^{\text{el}}, \quad (3.11)$$

where we have introduced Terzaghi's *effective* stress $\bar{\boldsymbol{\sigma}}$, and the *effective* chemical potentials $\bar{\mu}_{kK}$,

$$\bar{\boldsymbol{\sigma}} = \boldsymbol{\sigma} + p_W \mathbf{I}, \quad \bar{\mu}_{kK} = \mu_{kK} - \frac{p_W}{\rho_{kk}}, \quad k \in S^{\leftrightarrow}. \quad (3.12)$$

The constitutive relations take the form,

$$\bar{\boldsymbol{\sigma}} = \frac{\partial \mathcal{W}^{\text{el}}}{\partial \boldsymbol{\epsilon}^{\text{el}}}, \quad \bar{\mu}_{kS} = \frac{\partial \mathcal{W}^{\text{el}}}{\partial m_{kS}^{\text{el}}}, \quad k \in S^{\leftrightarrow}. \quad (3.13)$$

If we assume that transfer does not alter density, Eq. (2.9), equilibrium of the chemical potentials, i.e. $\mu_{kS} = \mu_{kW}$, is equivalent to equilibrium of the effective chemical potentials, i.e. $\bar{\mu}_{kS} = \bar{\mu}_{kW}$. Of course, equilibrium applies only for species that can cross the membrane.

3.4. Logarithmic isotropic hyperelasticity

Experimental data over a large range of stresses show that the elastic moduli of soils depend on the stress state. A usual approximation linked to the Cam–Clay models consists in assuming the elastic strain to be proportional to the logarithm of the mean-effective stress. Bolt (1956) has shown the influence of the chemical composition of pore water on the isotropic rebound (unloading) curves from high stresses: in the plane $\text{Ln}\bar{p}$ -void ratio e , they are almost linear trajectories emanating from a restricted zone with a very narrow range of void ratios. In our formulation, a constant chemical composition of the pore water is equivalent, if the pore pressure is constant, to a constant chemical potential of any species in fluid phase, and if the experiment is performed sufficiently slowly, to a constant chemical potential of any species that can cross the membrane. Thus, one would be lead a priori to use the effective stress and chemical potentials as primary variables. However, the formulation is facilitated if the effective stress and the masses of species in the solid phase $\{m_{kS}^{\text{el}}, k \in S^{\leftrightarrow}\}$ (or the molar fractions $\{x_{kS}^{\text{el}}, k \in S^{\leftrightarrow}\}$ defined consistently from the latter according to Eq. (2.17)) are considered as primary variables instead. From a practical point of view, the above mentioned unloading curves can be considered to occur at almost constant x_{kS}^{el} as mechanical loading, at constant chemical potential $\bar{\mu}_{kS}$, will be shown to have a small influence on the chemical composition of the solid phase.

Let us introduce the decomposition of the strain and total and effective stress tensors into their spherical and deviatoric parts, namely

$$\boldsymbol{\epsilon}^{\text{el}} = \frac{\text{tr} \boldsymbol{\epsilon}^{\text{el}}}{3} \mathbf{I} + \text{dev} \boldsymbol{\epsilon}^{\text{el}}, \quad \boldsymbol{\sigma} = -p \mathbf{I} + \mathbf{s}, \quad \bar{\boldsymbol{\sigma}} = -\bar{p} \mathbf{I} + \mathbf{s}, \quad (3.14)$$

with the two first stress-invariants

$$p = -\frac{\text{tr} \boldsymbol{\sigma}}{3}, \quad \bar{p} = -\frac{\text{tr} \bar{\boldsymbol{\sigma}}}{3}, \quad q = \left(\frac{3}{2} \mathbf{s} : \mathbf{s}\right)^{\frac{1}{2}}. \quad (3.15)$$

Let us consider now the purely chemical contribution to the chemo-elastic potential, namely $RT/V_0\varphi(\{x_{kS}^{\text{el}}, k \in S^{\leftrightarrow}\})$. We require this chemical part to have the classic form (2.7), that is since $N_{kK}^{\text{el}} = m_{kK}^{\text{el}}V_0/m_k^{(\text{M})}$, we require $\partial\varphi/\partial N_{kS}^{\text{el}} = \text{Ln}x_{kS}^{\text{el}}$. Then up to a constant depending on the number of moles of solid particles N_{cS} ,

$$\varphi(\{x_{kS}^{\text{el}}, k \in S^{\leftrightarrow}\}) = \sum_{k \in S^{\leftrightarrow}} N_{kS}^{\text{el}} \text{Ln} N_{kS}^{\text{el}} - \left(\sum_{l \in S} N_{lS}^{\text{el}} \right) \text{Ln} \left(\sum_{n \in S} N_{nS}^{\text{el}} \right). \quad (3.16)$$

We are now in position to obtain the chemo-elastic potential in the above motivated mixed form. For that purpose, we first define a partial Legendre transform $\mathcal{W}_M^{\text{el}}(\bar{\boldsymbol{\sigma}}, \{m_{kS}^{\text{el}}, k \in S^{\leftrightarrow}\})$ of the energy \mathcal{W}^{el} , namely

$$\delta\mathcal{W}_M^{\text{el}}(\bar{\boldsymbol{\sigma}}, \{m_{kS}^{\text{el}}, k \in S^{\leftrightarrow}\}) = \delta(\bar{\boldsymbol{\sigma}} : \boldsymbol{\epsilon}^{\text{el}} - \mathcal{W}^{\text{el}}) = \boldsymbol{\epsilon}^{\text{el}} : \delta\bar{\boldsymbol{\sigma}} - \sum_{k \in S^{\leftrightarrow}} \bar{\mu}_{kS} \delta m_{kS}^{\text{el}}, \quad (3.17)$$

from which follow the constitutive relations,

$$\boldsymbol{\epsilon}^{\text{el}} = \frac{\partial \mathcal{W}_M^{\text{el}}}{\partial \bar{\boldsymbol{\sigma}}}, \quad \bar{\mu}_{kS} = -\frac{\partial \mathcal{W}_M^{\text{el}}}{\partial m_{kS}^{\text{el}}}, \quad k \in S^{\leftrightarrow}. \quad (3.18)$$

In the analysis of Na-Montmorillonites (LHG, 2002) the dependence of elastic properties on chemical clay content could be reduced to the dependence on mass content (in fact the molar fraction) of absorbed water. In contrast, in heteroionic clays, there are several counterions in the solid phase to consider, with different impacts on clay deformation and deformability. Thus, the elastic properties are assumed to depend on the mass content in these counterions. So we set,

$$\mathcal{W}_M^{\text{el}}(\bar{\boldsymbol{\sigma}}, \{m_{kS}^{\text{el}}, k \in S^{\leftrightarrow}\}) = -\sum_{k \in S^{\leftrightarrow}} \mu_{kS}^0 m_{kS}^{\text{el}} - \bar{p} \text{tr} \boldsymbol{\epsilon}_k^{\text{el}} + \kappa F(\bar{p}, \bar{p}_k) + \frac{q^2}{6G} - \frac{RT}{V_0} \varphi, \quad (3.19)$$

where $\varphi = \varphi(x_{kS}^{\text{el}}, k \in S^{\leftrightarrow})$ and $\kappa = \kappa(x_{kS}^{\text{el}}, k \in S^+ \cup \{w\})$ and $\mu_{kS}^0 = g_{kS}^0/m_k^{(\text{M})}$, $k \in S^{\leftrightarrow}$. Here $F(\bar{p}, \bar{p}_k)$ is the function that introduces a logarithmic dependence in mean-stress,

$$F(\bar{p}, \bar{p}_k) = \bar{p} \text{Ln} \frac{\bar{p}}{\bar{p}_k} - \bar{p}, \quad \frac{dF}{d\bar{p}} = \text{Ln} \frac{\bar{p}}{\bar{p}_k}, \quad (3.20)$$

and $\text{tr} \boldsymbol{\epsilon}_k^{\text{el}}$ is the value of the elastic volume change when the effective mean-stress varies from the convergence stress \bar{p}_k to a small reference value \bar{p}_0 while the pore fluid is distilled water,

$$\text{tr} \boldsymbol{\epsilon}_k^{\text{el}} = -\kappa^{\text{dw}} \text{Ln} \frac{\bar{p}_k}{\bar{p}_0} \quad \text{with} \quad \kappa^{\text{dw}} = \kappa(x_{kS}^{\text{el,dw}}, k \in S^+ \cup \{w\}). \quad (3.21)$$

An estimation of the chemical content of clay clusters, denoted by the symbol dw, when pore water is distilled is proposed in Appendix D.

In absence of detailed experimental data showing the influence of the chemical composition of pore water on the shear modulus G , the latter will be simply assumed to be constant. Then, in view of the chemo-elastic potential (3.19), the elastic constitutive equations (3.18) reduce to:

$$\begin{cases} \boldsymbol{\epsilon}^{\text{el}} = \left(\text{tr} \boldsymbol{\epsilon}_k^{\text{el}} - \kappa \text{Ln} \frac{\bar{p}}{\bar{p}_k} \right) \frac{\mathbf{I}}{3} + \frac{\mathbf{s}}{2G}, \\ \bar{\mu}_{kS} = \mu_{kS}^0 - F(\bar{p}, \bar{p}_k) \frac{\partial \kappa}{\partial m_{kS}^{\text{el}}} + \frac{RT}{m_k^{(\text{M})}} \text{Ln} x_{kS}^{\text{el}}, \quad k \in S^{\leftrightarrow}. \end{cases} \quad (3.22)$$

Although the formulation is by no means restricted to such states, the manipulations will become more familiar to Cam–Clay users if the deviatoric stress and strain are assumed to maintain fixed directions during loading e.g. as for triaxial compression or extension paths, or more generally paths with constant Lode angle. Then the stress and strain states can be fully characterized by two work-conjugate invariants only, namely (\bar{p}, q) and $(\text{tr } \epsilon^{\text{el}}, \epsilon_q^{\text{el}})$. An incremental form of the elastic constitutive equations provides $(-\delta\bar{p}, \delta q, \{\delta\bar{\mu}_{kS}^{\text{ec}}, k \in S^{\leftrightarrow}\})$ in terms of $(\delta\text{tr } \epsilon^{\text{el}}, \delta\epsilon_q^{\text{el}}, \{\delta m_{kS}^{\text{el}}, k \in S^{\leftrightarrow}\})$. Note, however, that the masses are subject to the electroneutrality constraint, precluding the inversion of the above relations. On the other hand, inclusion of the electrical field as a Lagrangian in conjunction with *electro-chemical* potentials provides invertible constitutive equations via a symmetric matrix,

$$\begin{bmatrix} -\delta\bar{p} \\ \delta q \\ \delta\bar{\mu}_{wS}^{\text{ec}} \\ \delta\bar{\mu}_{NaS}^{\text{ec}} \\ \delta\bar{\mu}_{KS}^{\text{ec}} \\ \delta\bar{\mu}_{ClS}^{\text{ec}} \\ 0 \end{bmatrix} = \begin{bmatrix} B_{pp} & 0 & B_{pw} & B_{pNa} & B_{pK} & B_{pCl} & 0 \\ 0 & 3G & 0 & 0 & 0 & 0 & 0 \\ B_{wp} & 0 & \beta_{ww} & \beta_{wNa} & \beta_{wK} & \beta_{wCl} & 0 \\ B_{Nap} & 0 & \beta_{Naw} & \beta_{NaNa} & \beta_{NaK} & \beta_{NaCl} & \xi_{Na} \\ B_{Kp} & 0 & \beta_{Kw} & \beta_{KNa} & \beta_{KK} & \beta_{KCl} & \xi_K \\ B_{Clp} & 0 & \beta_{Clw} & \beta_{ClNa} & \beta_{CIK} & \beta_{ClCl} & \xi_{Cl} \\ 0 & 0 & 0 & \xi_{Na} & \xi_K & \xi_{Cl} & 0 \end{bmatrix} \begin{bmatrix} \delta\text{tr } \epsilon^{\text{el}} \\ \delta\epsilon_q^{\text{el}} \\ \delta m_{wS}^{\text{el}} \\ \delta m_{NaS}^{\text{el}} \\ \delta m_{KS}^{\text{el}} \\ \delta m_{ClS}^{\text{el}} \\ \delta\phi^S \end{bmatrix}. \quad (3.23)$$

Here the incremental bulk modulus B_{pp} and the coefficients B_{kp} , and β_{kl} , are defined as follows:

$$B_{pp} = \frac{\bar{p}}{\kappa}, \quad B_{pk} = B_{kp} = -\frac{\partial\bar{p}}{\partial m_{kS}^{\text{el}}} = \frac{\partial\bar{\mu}_{kS}^{\text{ec}}}{\partial\text{tr } \epsilon^{\text{el}}} = B_{pp} \ln \frac{\bar{p}}{\bar{p}_\kappa} \frac{\partial\kappa}{\partial m_{kS}^{\text{el}}}, \quad k \in S^{\leftrightarrow}, \quad (3.24)$$

and

$$\beta_{kl} = \beta_{lk} = \frac{\partial\bar{\mu}_{kS}^{\text{ec}}}{\partial m_{lS}^{\text{el}}} = \frac{B_{kp}B_{lp}}{B_{pp}} - F(\bar{p}, \bar{p}_\kappa) \frac{\partial^2\kappa}{\partial m_{kS}^{\text{el}} \partial m_{lS}^{\text{el}}} + \frac{RT}{m_k^{(\text{M})}} \frac{1}{x_{kS}^{\text{el}}} \frac{\partial x_{kS}^{\text{el}}}{\partial m_{lS}^{\text{el}}}, \quad k, l \in S^{\leftrightarrow}. \quad (3.25)$$

The symmetry of the β 's results from (2.18). Since the elastic shear modulus G is independent of the chemical composition of the solution, there is no coupling between shear components and chemical variables. In view of simplifying the notation in the elastic–plastic analysis, it will be convenient to denote the coefficients related to the shear components by

$$B_{qq} = 3G, \quad B_{kl} = 0, \quad (k, l) \neq (q, q). \quad (3.26)$$

The last line of (3.23) is obtained by differentiating the electroneutrality relation (2.24)₁: note that the latter is expressed in terms of total masses, but, when the behaviour is elastic, the changes of total and elastic masses coincide.

Notice that the symmetry of the incremental elastic stiffness is essentially due to the existence of the (electro-)chemo-elastic potential $\mathcal{W}_M^{\text{el}} + \sum_{k \in S^{\leftrightarrow}} \xi_k m_{kS}^{\text{el}} \phi^S$.

Remark 3.1. Identification of the pressures in the solid phase.

For incompressible species, the effective electro-chemical potentials of the species in the solid phase, Eqs. (2.17), (3.12), integrate to

$$\bar{\mu}_{kS}^{\text{ec}} = \mu_{kS}^{\text{ec}} - \frac{p_W}{\rho_{kS}} = \mu_{kS}^0 + \frac{p_{kS} - p_W}{\rho_{kS}} + \frac{RT}{m_k^{(\text{M})}} \ln x_{kS}^{\text{el}} + \xi_k \phi^S, \quad k \in S^{\leftrightarrow}. \quad (3.27)$$

Comparison with (3.22) gives the pressure difference $p_{kS} - p_W$ as a function of the variables $\bar{p}, \{m_{kS}^{\text{el}}, k \in S^{\leftrightarrow}\}$.

Remark 3.2. A strain-based chemo-elastic potential.

We have argued that extension to solutions containing many species would be easier if we use the above chemo-elastic potential in mixed form. One can nevertheless formally define a *strain-based* chemo-elastic potential $\mathcal{W}^{\text{el}}(\epsilon^{\text{el}}, \{m_{kS}^{\text{el}}, k \in S^{\leftrightarrow}\})$. Indeed, the effective mean-stress \bar{p} can be obtained from (3.22) as $\bar{p} = \bar{p}_\kappa \exp((\text{tr } \epsilon_k^{\text{el}} - \text{tr } \epsilon^{\text{el}})/\kappa)$. Substitution of the stress in $\mathcal{W}_M^{\text{el}}$ yields the strain-based chemo-elastic potential \mathcal{W}^{el} ,

$$\mathcal{W}^{\text{el}}(\epsilon^{\text{el}}, \{m_{kS}^{\text{el}}, k \in S^{\leftrightarrow}\}) = \sum_{k \in S^{\leftrightarrow}} \mu_{kS}^0 m_{kS}^{\text{el}} + \kappa \bar{p} + G \text{dev } \epsilon^{\text{el}} : \text{dev } \epsilon^{\text{el}} + \frac{RT}{V_0} \varphi, \quad (3.28)$$

where $\varphi = \varphi(x_{kS}^{\text{el}}, k \in S^{\leftrightarrow})$, $\kappa = \kappa(x_{kS}^{\text{el}}, k \in S^+ \cup \{w\})$. The constitutive equations follow via (3.13),

$$\begin{cases} \bar{\sigma} = -\bar{p}\mathbf{I} + 2G \text{dev } \epsilon^{\text{el}}, \quad \bar{p} = \bar{p}_\kappa \exp((\text{tr } \epsilon_k^{\text{el}} - \text{tr } \epsilon^{\text{el}})/\kappa), \\ \bar{\mu}_{kS}^{\text{cc}} = \mu_{kS}^0 - F(\bar{p}, \bar{p}_\kappa) \frac{\partial \kappa}{\partial m_{kS}^{\text{el}}} + \frac{RT}{m_k^{(M)}} \ln x_{kS}^{\text{el}} + \xi_k \phi^S, \quad k \in S^{\leftrightarrow}. \end{cases} \quad (3.29)$$

3.5. A simplified elastic model using the concept of chemical reaction

3.5.1. Cation exchange as a chemical reaction

In view of simplifying the above formalism, we now consider that the cations and adsorbed water do not affect the mechanical properties independently. We will employ constraint resulting from the chemical reaction analysis to express these relations of dependence.

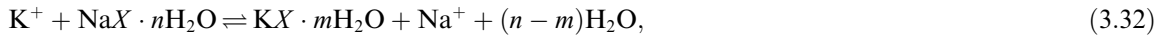
The amount of chloride anions in the solid phase is certainly small due to the presence of the negatively charged clay platelets. So, we may assume that the membrane is impermeable to chloride anions, or even that the number of moles of chloride anions is negligible,

$$N_{\text{CLS}} \simeq 0. \quad (3.30)$$

Therefore, if we account for the actual valences of the cations, $\zeta_{\text{Na}} = \zeta_{\text{K}} = 1$, the total number of exchangeable cations N_{ex} in the solid phase³ turns out to be constant, namely from (2.25),

$$N_{\text{NaS}}^{(\text{el})} + N_{\text{KS}}^{(\text{el})} = N_{\text{ex}} \equiv -\zeta_c N_{\text{cS}} = \text{constant} > 0, \quad (3.31)$$

where the superscript (el) is intended to imply that the relation is assumed to hold in terms of total numbers of cations, as well as in terms of the reversible change in their number. Consequently, a single variable is sufficient to describe the variation of the number of cations in the solid phase. Indeed, the cation exchange, combined with the mechanism of water absorption into/desorption from the clay crystal solid, may be viewed as a chemical reaction between solid and fluid phases,



involving

- the cations in pore water Na^+ and K^+ ,
- the exchange complex $\text{NaX} \cdot n\text{H}_2\text{O}$,
- absorbed or desorbed water, and
- n and m , stoichiometric numbers of moles of interlayer water hydrating a cation.

³ In fact, in the present analysis, N_{ex} can be considered either as the total number of cations in the solid phase or as the number of exchangeable cations.

Thus, the difference $n - m$ corresponds to the number of moles of water (per mole of clay) removed from/added to the solid phase as a result of the cation exchange: it introduces a second variable that describes the water content of the phases.

According to (3.32), the total and elastic changes in the numbers of moles of cations in the solid and fluid phases are linked by the following relations,

$$\delta N_{\text{NaS}}^{(\text{el})} = -\delta N_{\text{KS}}^{(\text{el})} = -\delta N_{\text{NaW}}^{\text{reactive}} = \delta N_{\text{KW}}^{\text{reactive}}. \quad (3.33)$$

Consequences for the relations between changes of (reversible) masses follow from the relation $m_{kK}^{(\text{el})} = m_k^{(\text{M})}/V_0 N_{kK}^{(\text{el})}$. The molar fractions of absorbed cations and water can be expressed in terms of the numbers of moles of cations Na^+ and of water,

$$x_{\text{NaS}}^{(\text{el})} = \frac{N_{\text{NaS}}^{(\text{el})}}{(1 - \zeta_c)N_{\text{cS}} + N_{\text{wS}}^{(\text{el})}}, \quad x_{\text{wS}}^{(\text{el})} = \frac{N_{\text{wS}}^{(\text{el})}}{(1 - \zeta_c)N_{\text{cS}} + N_{\text{wS}}^{(\text{el})}}. \quad (3.34)$$

Notice that $x_{\text{wS}}^{(\text{el})}$ depends on a single variable, namely on $N_{\text{wS}}^{(\text{el})}$.

3.5.2. Enthalpies of hydration and dehydration and the equilibrium constant

We shall consider in particular the smectite defined by $X = \text{Al}_3\text{Si}_3\text{O}_{10}(\text{OH})_2$ for which we have specific data available. If we restrict attention to the reaction of cation exchange, setting aside the absorption/desorption of water, the so-called equilibrium constant K_{eq} can be shown to be equal to the product of two terms, the first one coming from the mechanical contribution to the chemical potentials, the second one from the contribution due to the free enthalpies of hydration/dehydration,

$$K_{\text{eq}} = \frac{x_{\text{KS}}^{\text{el}}}{x_{\text{NaS}}^{\text{el}}} \frac{x_{\text{NaW}}}{x_{\text{KW}}} = \exp\left(-\frac{\Delta g^{\text{mech}}}{RT}\right) \exp\left(-\frac{\Delta g^{\text{hydr}}}{RT}\right). \quad (3.35)$$

To prove this relation, it will be convenient to use the effective mole-based chemical potentials $\bar{g}_{kS} = m_k^{\text{M}} \bar{\mu}_{kS}$, $k = \text{Na, K}$, and to choose the sole mass content of the sodium as independent variable. Let us start from the sum of incremental works done by the reversible changes of masses of the cations $\bar{\mu}_{kK} \delta m_{kK}^{\text{el}}$ with $k = \text{Na, K}$, and $K = \text{S, W}$. In this sum, all the incremental masses can be expressed in terms of $\delta m_{\text{NaS}}^{\text{el}}$, in view of (3.33). Hence, equilibrium is found to require that the mass-based chemical activities of the cations are the same in the solid and fluid phases, namely

$$\bar{A}_S - \bar{A}_W = 0, \quad (3.36)$$

with

$$\bar{A}_K = \frac{1}{m_{\text{Na}}^{(\text{M})}} (\bar{g}_{\text{NaK}} - \bar{g}_{\text{KK}}), \quad K = \text{S, W}. \quad (3.37)$$

The terms Δg^{mech} and Δg^{hydr} in Eq. (3.35) result from (3.36),

$$\Delta g^{\text{mech}} = \frac{m_{\text{Na}}^{(\text{M})}}{m_{\text{K}}^{(\text{M})}} \left(v_{\text{KS}}^{(\text{M})} p_{\text{KS}} - v_{\text{KW}}^{(\text{M})} p_{\text{W}} \right) - \left(v_{\text{NaS}}^{(\text{M})} p_{\text{NaS}} - v_{\text{NaW}}^{(\text{M})} p_{\text{W}} \right), \quad (3.38)$$

and

$$\Delta g^{\text{hydr}} = (g_{\text{KS}}^0 - g_{\text{NaS}}^0) - (g_{\text{KW}}^0 - g_{\text{NaW}}^0). \quad (3.39)$$

Here g_{KS}^0 is the free enthalpy of formation of the anhydrous part of the hydrated cluster $\text{KX} \cdot n\text{H}_2\text{O}$, with a similar definition for g_{NaS}^0 . g_{KW}^0 and g_{NaW}^0 are the free enthalpies of solubility of the cations K^+ and Na^+ in pore water.

The mechanical contribution to the equilibrium constant can be checked to be very small for the range of pressures of interest here, so that the first term on the rhs of (3.35) is practically equal to one.

For the smectite $\text{NaAl}_3\text{Si}_3\text{O}_{10}(\text{OH})_2$ under a pressure of 1 bar and at a temperature $T = 298$ °K, Tardy and Duplay (1992) provide the following data for the hydration free enthalpy $\Delta g^{\text{hydr}} = (-5591.1 - (-5565.9)) - (-282.5 - (-261.9)) = -4.6$ kJ/mol. The negative sign of this quantity implies the value of K_{eq} to be greater than 1, in fact $K_{\text{eq}} = 6.3$, and it indicates that the cation exchange from left to right in (3.32) is spontaneous.

3.5.3. Elastic constitutive equations

In view of the relations (3.30) and (3.33), the incremental elastic energy (3.17) simplifies to

$$\delta\mathcal{W}_M^{\text{el}}(\bar{\sigma}, \{m_{ws}^{\text{el}}, m_{NaS}^{\text{el}}\}) = \epsilon^{\text{el}} : \delta\bar{\sigma} - \bar{\mu}_{ws} \delta m_{ws}^{\text{el}} - \bar{A}_S \delta m_{NaS}^{\text{el}}, \quad (3.40)$$

from which follow the constitutive relations,

$$\epsilon^{\text{el}} = \frac{\partial\mathcal{W}_M^{\text{el}}}{\partial\bar{\sigma}}, \quad \bar{\mu}_{ws} = -\frac{\partial\mathcal{W}_M^{\text{el}}}{\partial m_{ws}^{\text{el}}}, \quad \bar{A}_S = -\frac{\partial\mathcal{W}_M^{\text{el}}}{\partial m_{NaS}^{\text{el}}}. \quad (3.41)$$

The elastic constitutive equations are thus completely defined as soon as the potential $\mathcal{W}_M^{\text{el}}$ is given, e.g. by (3.19). In fact, these equations can be viewed as a specialization of Eq. (3.22). Eq. (3.22)₁ remains unchanged as well as the chemical potential of absorbed water, Eq. (3.22)₂ for $k = w$. The only formal difference for the set of equations (3.22)₂ comes from the fact that the difference of partial derivatives $\partial/\partial m_{NaS}^{\text{el}} - m_K^{(M)}/m_{Na}^{(M)}\partial/\partial m_{KS}^{\text{el}}$ now becomes $\partial/\partial m_{NaS}^{\text{el}}$ in view of (3.33) as the dependence of κ on m_{NaS}^{el} and m_{KS}^{el} reduces to a dependence on m_{NaS}^{el} , so that

$$\bar{A}_S = \frac{1}{m_{Na}^{(M)}} (g_{NaK}^0 - g_{KK}^0) - F(\bar{p}, \bar{p}_K) \frac{\partial\kappa}{\partial m_{NaS}^{\text{el}}} + \frac{RT}{m_{Na}^{(M)}} \ln \frac{x_{NaS}^{\text{el}}}{x_{KS}^{\text{el}}}. \quad (3.42)$$

An incremental form of the elastic constitutive equations provides $(-\delta\bar{p}, \delta q, \delta\bar{\mu}_{ws}, \delta\bar{A}_S)$ in terms of $(\delta\text{tr}\epsilon^{\text{el}}, \delta\epsilon_q^{\text{el}}, \delta m_{ws}^{\text{el}}, \delta m_{NaS}^{\text{el}})$. In contrast to the general formulation of Section 3.4, the electroneutrality condition is now automatically accounted for and the electrical field need not to be involved. The incremental form of the elastic constitutive equations is then defined by a symmetric 4×4 matrix,

$$\begin{bmatrix} -\delta\bar{p} \\ \delta q \\ \delta\bar{\mu}_{ws} \\ \delta\bar{A}_S \end{bmatrix} = \begin{bmatrix} B_{pp} & 0 & B_{pw} & B_{pNa} \\ 0 & 3G & 0 & 0 \\ B_{wp} & 0 & \beta_{ww} & \beta_{wNa} \\ B_{Nap} & 0 & \beta_{Naw} & \beta_{NaNa} \end{bmatrix} \begin{bmatrix} \delta\text{tr}\epsilon^{\text{el}} \\ \delta\epsilon_q^{\text{el}} \\ \delta m_{ws}^{\text{el}} \\ \delta m_{NaS}^{\text{el}} \end{bmatrix}. \quad (3.43)$$

The coefficients B_{kl} and β_{kl} are still given by the formulas (3.24) and (3.25), to within the last term in (3.25).

4. Elastic–plastic constitutive equations

4.1. Scope of the model

The analysis presented in LHG (2002) was devoted to clays which contain essentially one cation, like the Ponza bentonite studied by Di Maio (1996) which is an essentially Na-Montmorillonite. The presence of several cations not only requires to account explicitly for electroneutrality but it also produces new aspects in the behaviour, as the relative contents of the two cations vary, as a consequence of the chemical composition of the pore water. These aspects have been introduced in the elastic behaviour through

κ -dependence in the molar fractions of the cations. However, experimental data available so far in the literature do not reveal effects on the plastic behaviour typical of the presence of several cations. Therefore, the elastic–plastic model will follow the same trend as for Na-Montmorillonites, to within the fact that the relative contents of the cations will be kept trace of. The main features of the elastic–plastic behaviour that we want to model are motivated first by the experimental observations of Di Maio and Onorati (1999) on Bisaccia clay, a clay of marine origin.

4.1.1. Mechanical loading

The specimen is in contact with a large reservoir of constant chemical composition and at atmospheric pressure, so that $p_w \sim 0$. The load is continuously varied, sufficiently slowly however in such a way that electro-chemical equilibrium can be established at the end of each load increment. Therefore, one may assume the electro-chemical potentials of all species that can transfer to be equal, at the end of each load increment, to the known electro-chemical potentials of their counterparts in pore water. Experiments show that the curves $e - \ln \bar{p}$ are approximately straight and converging to a small void ratio interval. However, the slopes of the loading and unloading curves decrease as the Na-content of the pore water increases. This trend holds whatever this content, that is from zero Na-content (distilled water) to saturated solutions (that is at 20 °K and under atmospheric pressure, 6.15 moles of NaCl per liter of water).

4.1.2. Chemical loading: chemical consolidation and swelling

Under constant mechanical conditions, a chemical loading consists in varying the Na-content, or K-content, of the pore water. When the latter increases, the void ratio decreases, and this decrease rate is especially large at small salt content. When the specimen is re-exposed to distilled water, its volume increases. These volume changes are in qualitative agreement with the osmotic effect: increase of salt content leads to an increase of pore water pressure, and this in turn leads to water desorption. Alternatively, one may say that water desorption/absorption occurs to equilibrate the salt contents in pore water and clay pockets.

4.1.3. Elastic and elastic–plastic behaviours: chemical softening and preconsolidation

Mechanical loading at constant chemical composition corresponds clearly to an elastic–plastic behaviour while mechanical unloading can be conjectured to be purely elastic, see Fig. 8 of Di Maio (1996). The situation is more complex for chemical loadings. At relatively small stresses, chemical loading cycles on Ponza Bentonite (void ratio between 1 and 8) seem to be practically reversible while the amount of plastic contractancy increases with the applied stress, Fig. 7 of Di Maio (1996).

However, mechanical loading following chemical consolidation was observed to give rise to preconsolidation on reconstituted specimens of Bisaccia clay (void ratio between 1 and 3), Fig. 7 of Di Maio and Fenelli (1997).

During chemical loading on normally consolidated materials, the elastic–plastic model developed in LHG (2002) and adapted here to the presence of two cations shows first an elastic–plastic behaviour followed by an elastic behaviour, thus displaying both plasticity and preconsolidation due to chemical effects. The relative importance of the plastic stage increases with confining stresses. In a simplified version of the model, chemical loading on normally consolidated materials occurs in the elastic regime.

The behaviour qualitatively described above is now given an analytic expression.

4.2. Incremental elastic–plastic relations

4.2.1. The general case of compressible species

The generalized strains are decomposed in an elastic part (superscript el) and a plastic part (superscript pl), namely

$$\boldsymbol{\epsilon} = \boldsymbol{\epsilon}^{\text{el}} + \boldsymbol{\epsilon}^{\text{pl}}, \quad v_W = v_W^{\text{el}} + v_W^{\text{pl}}, \quad m_{kS} = m_{kS}^{\text{el}} + m_{kS}^{\text{pl}}, \quad k \in S^{\leftrightarrow}. \quad (4.1)$$

The plastic incremental flow relations are motivated by the dissipation inequality (3.7)₁. In fact, let us first substitute $\delta\Psi^{\text{el}}$ by $\delta\Psi_W^{\text{el}} + \delta\mathcal{W}^{\text{el}}$ using (2.30) and (3.9), and second let us use the strain decomposition (4.1). The resulting dissipation δD_1 ,

$$\delta D_1 = \boldsymbol{\sigma} : \delta\boldsymbol{\epsilon}^{\text{pl}} + p_W \delta v_W^{\text{pl}} + \sum_{k \in S^{\leftrightarrow}} \mu_{kS} \delta m_{kS}^{\text{pl}} \geq 0, \quad (4.2)$$

motivates the generalized normality flow rule,

$$\delta\boldsymbol{\epsilon}^{\text{pl}} = \delta\Lambda \frac{\partial g}{\partial \boldsymbol{\sigma}}, \quad \delta v_W^{\text{pl}} = \delta\Lambda \frac{\partial g}{\partial p_W}, \quad \delta m_{kS}^{\text{pl}} = \delta\Lambda \frac{\partial g}{\partial \mu_{kS}}, \quad k \in S^{\leftrightarrow}, \quad (4.3)$$

where $\delta\Lambda \geq 0$ is the plastic multiplier and $g = g(\boldsymbol{\sigma}, p_W, \{\mu_{kS}, k \in S^{\leftrightarrow}\})$ the plastic potential.

4.2.2. Incompressible species

Henceforth, the analysis is restricted to incompressible species. The incompressibility constraint (2.32), that holds in both the elastic and elastic–plastic regimes, provides the increment of plastic volume change of the fluid phase,

$$\delta v_W^{\text{pl}} = \delta \text{tr} \boldsymbol{\epsilon}^{\text{pl}} - \sum_{k \in S^{\leftrightarrow}} \frac{\delta m_{kS}^{\text{pl}}}{\rho_{kS}}. \quad (4.4)$$

The dissipation inequality (4.2) becomes

$$\delta D_1 = \bar{\boldsymbol{\sigma}} : \delta\boldsymbol{\epsilon}^{\text{pl}} + \sum_{k \in S^{\leftrightarrow}} \bar{\mu}_{kS} \delta m_{kS}^{\text{pl}} = -\bar{p} \text{tr} \delta\boldsymbol{\epsilon}^{\text{pl}} + \mathbf{s} : \text{dev} \delta\boldsymbol{\epsilon}^{\text{pl}} + \sum_{k \in S^{\leftrightarrow}} \bar{\mu}_{kS} \delta m_{kS}^{\text{pl}} \geq 0. \quad (4.5)$$

If, for simplicity, the analysis is restricted to stress paths with constant Lode angles, that expression motivates the generalized normality flow rule

$$\text{tr} \delta\boldsymbol{\epsilon}^{\text{pl}} = -\delta\Lambda \frac{\partial g}{\partial \bar{p}}, \quad \text{dev} \delta\boldsymbol{\epsilon}^{\text{pl}} = \delta\Lambda \frac{\partial g}{\partial q} \frac{3}{2} \frac{\mathbf{s}}{q}, \quad \delta m_{kS}^{\text{pl}} = \delta\Lambda \frac{\partial g}{\partial \bar{\mu}_{kS}}, \quad k \in S^{\leftrightarrow}. \quad (4.6)$$

Notice that in general the plastic increment of volume change of the fluid phase (4.4) has no reason to vanish: in fact, it has been introduced specifically in order the incompressibility condition be satisfied. Its existence in the compressible case allows a smooth transition between compressible and incompressible materials.

4.2.3. Mechanical and chemical hardening/softening

The lines of volume changes during mechanical loadings have a slope $\lambda(\bar{\mu}_{kS}, k \in S^+ \cup \{W\})$ and converge to a point \bar{p}_λ ,

$$\text{tr} \boldsymbol{\epsilon} = \text{tr} \boldsymbol{\epsilon}_\lambda - \lambda(\bar{\mu}_{kS}, k \in S^+ \cup \{W\}) \ln \frac{\bar{p}}{\bar{p}_\lambda}, \quad \text{tr} \boldsymbol{\epsilon}_\lambda = -\lambda^{\text{dw}} \ln \frac{\bar{p}_\lambda}{\bar{p}_0}, \quad (4.7)$$

while the unloading curves emanate a priori from a different point \bar{p}_κ , Eqs. (3.21), (3.22),

$$\text{tr} \boldsymbol{\epsilon}^{\text{el}} = \text{tr} \boldsymbol{\epsilon}_\kappa^{\text{el}} - \kappa(x_{kS}^{\text{el}}, k \in S^+ \cup \{W\}) \ln \frac{\bar{p}}{\bar{p}_\kappa}, \quad \text{tr} \boldsymbol{\epsilon}_\kappa^{\text{el}} = -\kappa^{\text{dw}} \ln \frac{\bar{p}_\kappa}{\bar{p}_0}, \quad (4.8)$$

with $\lambda^{\text{dw}} = \lambda(\bar{\mu}_{kS}^{\text{dw}}, k \in S^+ \cup \{W\})$, $\kappa^{\text{dw}} = \kappa(x_{kS}^{\text{el,dw}}, k \in S^+ \cup \{W\})$. Combining these two relations provides the preconsolidation stress p_c . In order to reduce the chemical dependence of p_c to a single type of parameter,

namely the chemical potentials, we introduce a slight qualitative modification, expressing the chemical dependence of κ as $\tilde{\kappa} = \tilde{\kappa}(\bar{\mu}_{ks}, k \in S^+ \cup \{w\})$. The resulting preconsolidation stress,

$$(\lambda - \tilde{\kappa}) \ln \frac{p_c}{\bar{p}_0} = -\text{tr} \epsilon^{\text{pl}} + ((\lambda - \tilde{\kappa}) - (\lambda^{\text{dw}} - \tilde{\kappa}^{\text{dw}})) \ln \frac{\bar{p}_\lambda}{\bar{p}_0} + (\tilde{\kappa} - \tilde{\kappa}^{\text{dw}}) \ln \frac{\bar{p}_\lambda}{\bar{p}_\kappa}, \quad (4.9)$$

with differential

$$(\lambda - \tilde{\kappa}) \frac{\delta p_c}{p_c} = -\delta \text{tr} \epsilon^{\text{pl}} + \ln \frac{\bar{p}_\lambda}{p_c} \delta \lambda - \ln \frac{\bar{p}_\kappa}{p_c} \delta \tilde{\kappa}, \quad (4.10)$$

appears as a modification of the usual Cam–Clay expression, which is recovered when both $\bar{p}_\kappa = \bar{p}_\lambda$ and $\lambda - \tilde{\kappa}$ is independent of chemical content of the solid phase.

4.2.4. Incremental relations

We now specialize (4.6) and, following the arguments above, the plastic potential g and the yield function f will be assumed to depend only on $\bar{p}, q, \{\bar{\mu}_{ks}, k \in S^+ \cup \{w\}\}$, and on $\text{tr} \epsilon^{\text{pl}}$, which allows for hardening or softening. For plastic loading, that is the stress point is on the yield surface and stays there, $f = 0$ and $\delta f = 0$, the incremental constitutive equations become,

$$\begin{bmatrix} -\delta \bar{p} \\ \delta q \\ \delta \bar{\mu}_{ws}^{\text{ec}} \\ \delta \bar{\mu}_{nas}^{\text{ec}} \\ \delta \bar{\mu}_{ks}^{\text{ec}} \\ \delta \bar{\mu}_{cls}^{\text{ec}} \\ 0 \end{bmatrix} = \begin{bmatrix} B_{pp}^{\text{ep}} & B_{pq}^{\text{ep}} & B_{pw}^{\text{ep}} & B_{pNa}^{\text{ep}} & B_{pK}^{\text{ep}} & B_{pCl}^{\text{ep}} & 0 \\ B_{qp}^{\text{ep}} & B_{qq}^{\text{ep}} & B_{qw}^{\text{ep}} & B_{qNa}^{\text{ep}} & B_{qK}^{\text{ep}} & B_{qCl}^{\text{ep}} & 0 \\ B_{wp}^{\text{ep}} & B_{wq}^{\text{ep}} & \beta_{ww}^{\text{ep}} & \beta_{wNa}^{\text{ep}} & \beta_{wK}^{\text{ep}} & \beta_{wCl}^{\text{ep}} & 0 \\ B_{Nap}^{\text{ep}} & B_{Naq}^{\text{ep}} & \beta_{Naw}^{\text{ep}} & \beta_{NaNa}^{\text{ep}} & \beta_{NaK}^{\text{ep}} & \beta_{NaCl}^{\text{ep}} & \xi_{Na} \\ B_{Kp}^{\text{ep}} & B_{Kq}^{\text{ep}} & \beta_{Kw}^{\text{ep}} & \beta_{KNa}^{\text{ep}} & \beta_{KK}^{\text{ep}} & \beta_{KCl}^{\text{ep}} & \xi_K \\ B_{Clp}^{\text{ep}} & B_{Clq}^{\text{ep}} & \beta_{Clw}^{\text{ep}} & \beta_{ClNa}^{\text{ep}} & \beta_{CIK}^{\text{ep}} & \beta_{ClCl}^{\text{ep}} & \xi_{Cl} \\ 0 & 0 & 0 & \xi_{Na} & \xi_K & \xi_{Cl} & 0 \end{bmatrix} \begin{bmatrix} \delta \text{tr} \epsilon \\ \delta \epsilon_q \\ \delta m_{ws} \\ \delta m_{nas} \\ \delta m_{ks} \\ \delta m_{cls} \\ \delta \phi^S \end{bmatrix}. \quad (4.11)$$

The incremental moduli B_{kl}^{ep} and β_{kl}^{ep} differ from their elastic counterparts B_{kl} which can be read from (3.23), and β_{kl} , Eq. (3.25), by a dyadic product, namely:

$$B_{kl}^{\text{ep}} = B_{kl} - \frac{1}{H} g_k f_l, \quad k, l \in \{p, q, S^\leftrightarrow\}, \quad (4.12)$$

and

$$\beta_{kl}^{\text{ep}} = \beta_{kl} - \frac{1}{H} g_k f_l, \quad k, l \in S^\leftrightarrow. \quad (4.13)$$

The general expressions of the coefficients entering in (4.11), namely $f_k, g_k, k \in \{p, q, S^\leftrightarrow\}$, of the plastic modulus $H > 0$ and the hardening modulus h are reported in Appendix B, together with their specializations when the yield function and plastic potential are of the Modified Cam–Clay type, namely

$$f = f(\bar{p}, q, \{\bar{\mu}_{ks}, k \in S^+ \cup \{w\}\}, \text{tr} \epsilon^{\text{pl}}) = \frac{q^2}{M^2 \bar{p}} + \bar{p} - p_c, \quad (4.14)$$

with $M = M(\bar{\mu}_{ks}, k \in S^+ \cup \{w\})$ and $p_c = p_c(\{\bar{\mu}_{ks}, k \in S^+ \cup \{w\}\}, \text{tr} \epsilon^{\text{pl}})$. Notice that the major symmetry of the elastic–plastic incremental relations holds iff the flow rule is associative, namely $f = g$.

Remark 4.1. The simplified model without chemical preconsolidation.

When the difference $\lambda - \kappa$ is constant and the effective mean-stresses \bar{p}_κ and \bar{p}_λ are equal, the preconsolidation stress p_c , Eqs. (4.9), (4.10), does not depend on the chemical effects. Chemical loadings and unloadings are then elastic, Fig. 3 of LHG (2002). Furthermore, the incremental response to isotropic paths

simplifies, since then f and g do not depend on the chemical potentials: $\delta q = 0$, $\delta \epsilon_q = 0$, and, for the associative Modified Cam–Clay (4.14),

$$B_{kp}^{\text{ep}} = \frac{\kappa}{\lambda} B_{kp}, k \in \{p, S^{\leftrightarrow}\}, \quad \beta_{kl}^{\text{ep}} = \beta_{kl} - \frac{1}{H} B_{kp} B_{lp}, k, l \in S^{\leftrightarrow}, \quad (4.15)$$

with

$$H = \left(\frac{1}{\lambda - \kappa} + \frac{1}{\kappa} \right) \bar{p}. \quad (4.16)$$

4.2.5. The simplified elasto-plastic model using the concept of chemical reaction

The formulation is now specialized using the concept of chemical reaction in line with the development of Section 3.5.

Satisfying the relation (3.31) for both the elastic and total number of moles of cations requires the variations of the elastic and plastic (i.e. irreversible) numbers of moles of cations to be opposite,

$$\delta N_{\text{NaS}}^{pl} + \delta N_{\text{KS}}^{pl} = 0. \quad (4.17)$$

Therefore the dissipation inequality (4.5) becomes,

$$\delta D_1 = -\bar{p} \text{tr} \delta \epsilon^{\text{pl}} + \mathbf{s} : \text{dev} \delta \epsilon^{\text{pl}} + \bar{\mu}_{ws} \delta m_{ws}^{\text{pl}} + \bar{A}_s \delta m_{\text{NaS}}^{\text{pl}} \geq 0. \quad (4.18)$$

If, for simplicity, the analysis is restricted to stress paths with constant Lode angles, that expression motivates the generalized normality flow rule

$$\text{tr} \delta \epsilon^{\text{pl}} = -\delta \Lambda \frac{\partial g}{\partial \bar{p}}, \quad \text{dev} \delta \epsilon^{\text{pl}} = \delta \Lambda \frac{\partial g}{\partial q} \frac{3}{2} \frac{\mathbf{s}}{q}, \quad \delta m_{ws}^{\text{pl}} = \delta \Lambda \frac{\partial g}{\partial \bar{\mu}_{ws}}, \quad \delta m_{\text{NaS}}^{\text{pl}} = \delta \Lambda \frac{\partial g}{\partial \bar{A}_s}, \quad (4.19)$$

with the generalized potential $g = g(\bar{p}, q, \bar{\mu}_{ws}, \bar{A}_s)$. The yield function f has the same arguments as g plus $\text{tr} \epsilon^{\text{pl}}$ which allows for hardening and softening.

The calibrations of typical interpolation functions for λ and M in terms of $\{\bar{\mu}_{ws}, \bar{A}_s\}$ are provided in Appendix C.

5. Simulations of chemo-mechanical processes

The subsequent simulations aim at quantifying the ability of the simplified model using the concept of chemical reaction to capture the main features of the chemo-mechanical couplings that have been described in Section 4.1. For that purpose, it would be desirable to have available a series of experiments on homogeneous specimens. A key difficulty stems from the time duration necessary to perform chemical loadings for which chemical equilibrium can be considered to hold at any time. States at which macro-transport processes have become steady at desired concentrations deemed uniform throughout the specimen are considered only. An order of magnitude of the duration the physico-chemical processes need to reach equilibrium can be grasped from the chemical tests at fixed mean-stresses shown in Figs. 5(a) and 8(a). They refer to oedometric tests on cylindrical specimens of initial height 20 mm. However for the sake of simplification, they are used as isotropic tests for parameter calibration and subsequent simulations. Chemical consolidation appears to reach equilibrium in few days, while swelling is a much slower process, requiring several weeks. The experimental data used here are assumed to represent effectively a succession of equilibrium states, that is, with reference to the simplified model,

$$\bar{\mu}_{ws} = \bar{\mu}_{ww}, \quad \bar{A}_s = \bar{A}_w. \quad (5.1)$$

5.1. Model calibration

The behaviour of Ponza bentonite, an essentially Na-montmorillonite clay, is explained by the one-salt model exposed in LHG (2002). Part of the behaviour of Bisaccia clay, a natural marine-origin clay, is explained by this model as well when it is exposed to distilled water or saline solutions of NaCl only. However, when chemical loading involves another salt, it is necessary to have a finer description of the solid phase. In line with the present modeling, Bisaccia clay will be considered to contain two essential cations, Na^+ and K^+ . The directly measurable material parameters of these clays are reported in Table 1 and the resulting model coefficients are provided in Table 2.

The compliances $\kappa (= \tilde{\kappa})$ and λ are defined through a double interpolation between two sets of extreme situations, as detailed in Appendix A and in Appendix C respectively. One interpolation is based on the chemical potential of absorbed water as in LHG (2002). The second interpolation is based on the chemical activity. Indeed, we consider in turn the two hypothetical extreme situations where the molar fraction of one cation, say cation Na^+ , overweights the other in both phases. Let us give a flavour of the procedure for the elastic–plastic compliance λ . In reference to Fig. 2, the corresponding states are referred to as belonging to the Na-plane and λ is noted λ_{Na} . We measure $\lambda_{\text{Na}}^{\text{dw}}$ and $\lambda_{\text{Na}}^{\text{sat}}$ corresponding respectively to distilled water and NaCl-saturated solution. The chemical effect on λ_{Na} is introduced through a first interpolation between these two situations, for example

$$\lambda_{\text{Na}}(\bar{\mu}_{\text{ws}}) = \lambda_{1\text{Na}}\Phi(\lambda_{3\text{Na}}\theta_{\text{Na}}(\bar{\mu}_{\text{ws}})) + \lambda_{2\text{Na}}, \quad (5.2)$$

where the $\lambda_{i\text{Na}}$'s, $i = 1, 3$, are constants and Φ and θ_{Na} two interpolation functions.

The same procedure is followed to define the $\lambda_{i\text{K}}$'s, $i = 1, 3$. Next, a second interpolation is defined between the two reference planes, namely Na-plane and K-plane, based on the weights $\tilde{\omega}_k$, $k = \text{Na}, \text{K}$, Eq. (C.8), namely

$$\lambda = \lambda_1\Phi(\lambda_3\theta) + \lambda_2, \quad (5.3)$$

with

$$\lambda_1 = \sum_{k=\text{Na}, \text{K}} \tilde{\omega}_k \lambda_{1k}, \quad \lambda_2 = \sum_{k=\text{Na}, \text{K}} \tilde{\omega}_k \lambda_{2k}, \quad \lambda_3\theta(\bar{\mu}_{\text{ws}}) = \sum_{k=\text{Na}, \text{K}} \tilde{\omega}_k \lambda_{3k} \theta_k(\bar{\mu}_{\text{ws}}). \quad (5.4)$$

These weights, which are linked to the chemical activity, Eq. (C.9)₁, are based on the relative numbers of moles of the cations sodium and potassium.

The Ponza bentonite and Bisaccia clay have been remolded using distilled water and later exposed to various saline pore solutions. During mechanical loading, the samples are assumed to remain in contact with their initial pore solution; however even if they are exposed to distilled water during the mechanical

Table 1
Material parameters

Material	$\kappa_{\text{Na}}^{\text{dw}}$	$\kappa_{\text{Na}}^{\text{sat}}$	$\lambda_{\text{Na}}^{\text{dw}}$	$\lambda_{\text{Na}}^{\text{sat}}$	$\kappa_{\text{K}}^{\text{dw}}$	$\kappa_{\text{K}}^{\text{sat}}$	$\lambda_{\text{K}}^{\text{dw}}$	$\lambda_{\text{K}}^{\text{sat}}$
Bisaccia clay	0.120	0.010	0.200	0.090	0.013	0.005	0.093	0.085
Ponza bentonite	0.081	0.011	0.171	0.101	0.020	0.014	0.110	0.104

Table 2
Model coefficients

Material	$\kappa_{1\text{Na}}$	$\kappa_{3\text{Na}}$	$\lambda_{1\text{Na}}$	$\lambda_{3\text{Na}}$	$\kappa_{1\text{K}}$	$\kappa_{3\text{K}}$	$\lambda_{1\text{K}}$	$\lambda_{3\text{K}}$	K_{eq}	\bar{p}_{κ} (kPa)	\bar{p}_{λ} (kPa)
Bisaccia clay	-0.11	3.5	-0.11	6.0	-0.008	3.5	-0.008	6.0	5.0	800	800
Ponza bentonite	-0.07	6.0	-0.07	6.0	-0.006	6.0	-0.006	6.0	5.0	1400	2600

Table 3

Initial conditions and other physical data

Material	e_0	p_{c0} (kPa)	N_{cs}	N_{ws}	N_{nas}	N_{ks}	N_{ww}	$1 - x_{ww}$	ζ_c
Bisaccia clay	3.30	10	1570	21,100	278	245	21,100	10^{-6}	-0.33
Ponza bentonite	8.00	40	1570	21,100	491.4	31.9	81,446	10^{-6}	-0.33

loading, the duration of the mechanical test is so small that a chemical loading which involves a diffusion process has no time to take place.

Initial conditions are obtained as described in Appendix D with $\alpha = 0$. The corresponding numbers of moles for one cubic meter of porous media are given in Table 3. The chemical content of pore water is obtained from Eq. (D.7). At 20 °K, water saturation by the sole NaCl is reached for $x_{NaW}^{\text{sat}} = 0.091$, and water saturation by the sole KCl is $x_{Kw}^{\text{sat}} = 0.078$. Saturation in presence of the two salts is not experienced in the simulations reported here.

In fact, not all the measurable quantities listed in Table 1 are available. Practically, the identification procedure is skewed by the fact that there are many more data in or close to the Na-plane than to the K-plane. In the Na-plane, the parameters corresponding to both distilled pore water and NaCl-saturated solution are available, that is measurable directly from the stress-strain curves or through slopes. The other parameters are either guessed or defined in order to satisfy some qualitative specification as described below. Partial information grasped from experimental data indicates that the presence of cations K^+ in the solid phase stiffens the mechanical behaviour, that is, it reduces significantly the compliances κ and λ .

In LHG (2002), it was observed that chemical loading and unloading at constant stress are purely elastic processes if the difference $\lambda - \tilde{\kappa}$ is constant while the limit mean-stresses \bar{p}_κ and \bar{p}_λ are equal. In fact, this follows from (4.10) which then simplifies to

$$(\lambda - \tilde{\kappa}) \frac{\delta p_c}{p_c} = -\delta \text{tr} \epsilon^{\text{pl}} + \ln \frac{\bar{p}_\lambda}{p_c} \delta(\lambda - \tilde{\kappa}). \quad (5.5)$$

Clearly, for $\lambda - \tilde{\kappa}$ constant, the preconsolidation stress is not affected by changes of the chemical state. However, some experiments by Di Maio (1996) show that chemical loading cycles are accompanied with irreversible strains, whose intensity increases with the mean-stress level. Consequently, $\lambda - \tilde{\kappa}$ should depend in general on the chemical state, which for homoionic clays, is defined by the chemical potential of water $\bar{\mu}_{ws}$. One may expect the chemical activity of the cations to be involved as well for heteroionic clays.

In order to analyze the chemical influence on p_c , let us consider temporarily a simplified setting. The functions θ_k , $k = \text{Na, K}$, Eq. (5.2), which introduce the dependence with respect to the chemical potential of absorbed water $\bar{\mu}_{ws}$, are taken to be the same for both cations, that is

$$\kappa_{3k} = \kappa_3, \quad \lambda_{3k} = \lambda_3, \quad \theta_k(\bar{\mu}_{ws}) = \theta(\bar{\mu}_{ws}) \quad \text{for } k = \text{Na, K}. \quad (5.6)$$

The dependence of $\lambda - \tilde{\kappa}$ with respect to the chemical potential of absorbed water and to the chemical activity can be identified via (5.2)–(5.4),

$$d(\lambda - \tilde{\kappa}) = \frac{\partial(\lambda - \tilde{\kappa})}{\partial \tilde{\omega}_{\text{Na}}} d\tilde{\omega}_{\text{Na}} + \frac{\partial(\lambda - \tilde{\kappa})}{\partial \bar{\mu}_{ws}} d\bar{\mu}_{ws}, \quad (5.7)$$

where

$$\frac{\partial(\lambda - \tilde{\kappa})}{\partial \tilde{\omega}_{\text{Na}}} = (\lambda_{1\text{Na}} - \lambda_{1\text{K}})\Phi(\lambda_3\theta) - (\kappa_{1\text{Na}} - \kappa_{1\text{K}})\Phi(\kappa_3\theta) + (\lambda_{\text{Na}}^{\text{dw}} - \lambda_{\text{K}}^{\text{dw}}) - (\kappa_{\text{Na}}^{\text{dw}} - \kappa_{\text{K}}^{\text{dw}}), \quad (5.8)$$

and

$$\frac{\partial(\lambda - \tilde{\kappa})}{\partial \bar{\mu}_{ws}} = (\lambda_1\lambda_3\Phi'(\lambda_3\theta) - \kappa_1\kappa_3\Phi'(\kappa_3\theta)) \frac{d\theta}{d\bar{\mu}_{ws}}. \quad (5.9)$$

Then the coefficient of the chemical activity in (5.7) vanishes, and only the chemical potential of absorbed water influences p_c , if the material coefficients satisfy the following restrictions,

$$\lambda_{\text{Na}}^{\text{sat}} - \kappa_{\text{Na}}^{\text{sat}} = \lambda_{\text{K}}^{\text{sat}} - \kappa_{\text{K}}^{\text{sat}}, \quad \lambda_{\text{Na}}^{\text{dw}} - \kappa_{\text{Na}}^{\text{dw}} = \lambda_{\text{K}}^{\text{dw}} - \kappa_{\text{K}}^{\text{dw}}, \quad \lambda_{3\text{Na}} = \lambda_{3\text{K}} = \kappa_{3\text{Na}} = \kappa_{3\text{K}}. \quad (5.10)$$

If in addition, $\lambda_1 = \kappa_1$, that is, if

$$\lambda_{\text{Na}}^{\text{sat}} - \kappa_{\text{Na}}^{\text{sat}} = \lambda_{\text{K}}^{\text{sat}} - \kappa_{\text{K}}^{\text{sat}} = \lambda_{\text{Na}}^{\text{dw}} - \kappa_{\text{Na}}^{\text{dw}} = \lambda_{\text{K}}^{\text{dw}} - \kappa_{\text{K}}^{\text{dw}}, \quad \lambda_{3\text{Na}} = \lambda_{3\text{K}} = \kappa_{3\text{Na}} = \kappa_{3\text{K}}, \quad (5.11)$$

there is no chemical influence any longer on p_c and therefore chemical loadings and unloadings at constant effective stress are elastic, if $\bar{p}_\lambda = \bar{p}_\kappa$.

However, in LHG (2002), the values of $\kappa_{3\text{Na}}$ and $\lambda_{3\text{Na}}$, which can be identified as chemical consolidation/swelling slopes, Eq. (C.5), were shown to be distinct for Bisaccia Clay. On the other hand, in absence of available data, we shall accept the constraints (5.6)_{1,2} which require that these slopes are the same for the Na- and K-planes of Fig. 2. In addition, we do not have specific data that allow to explore the intensity of plasticity for paths at constant chemical activity and at constant chemical potential of water respectively. Therefore, we shall accept that the distance between the elastic and plastic coefficients is a constant in the Na- and K-planes, and that this constant is the same in these two planes as indicated by the first set of equalities in (5.11).

For Ponza bentonite, the identification procedure of LHG (2002) provides parameters on the Na-plane that verify the related constraints dictated by (5.11). The parameters in the K-plane are chosen in order that all the relations in (5.11) be satisfied. However, plasticity during purely chemical loadings can occur if the limit stresses \bar{p}_κ and \bar{p}_λ are not equal.

The first set of equalities in (5.11) leaves a single value to be ascribed for the parameters in the K-plane, say $\lambda_{\text{K}}^{\text{dw}}$. After the initial state corresponding to distilled water has been obtained in the solid phase, the parameter $\lambda_{\text{K}}^{\text{dw}}$ can be calculated using the interpolation rules since the corresponding elastic–plastic slope is available.

5.2. Mechanical and chemical loading cycles

In order to highlight the strong effects of chemical loading, the evolution of the void ratio for the specimen which is in contact with distilled water and undergoes a purely mechanical loading is used as a reference, marked by dashed curves in Fig. 3.

Fig. 3 shows mixed chemo-mechanical loading and unloading cycles. The mechanical load is the effective mean-stress while the chemical load is the molar fraction of NaCl in pore water. The simulated consolidation curves are nearly straight. The three tests in Fig. 3 differ by the values of the effective mean-stresses at which the chemical loadings (replacement of distilled pore water by NaCl-saturated solution) and unloadings (return to a distilled pore-water solution) take place.

Since $\lambda - \tilde{\kappa}$ is not constant, chemical loading leads first to a change, in fact a decrease, of the preconsolidation stress p_c , a phenomenon that can be referred to as *chemical softening*. Thus plasticity occurs to compensate for this negative effect and to maintain the preconsolidation stress equal to the applied stress, up to a point from which the chemical influence on p_c becomes positive, i.e. p_c increases due to the increase of Na^+ in solid phase, leading to *chemical hardening* and preconsolidation, Fig. 7(a). Plasticity gives rise to an increased chemical consolidation. During chemical unloading, the swelling is partly elastic and partly elastic–plastic, as can be checked from Fig. 7(b). The volume change is larger than during chemical consolidation, and in this respect the behaviour of Bisaccia clay is quite distinct from that of Ponza bentonite. Indeed for the latter, the void ratio at the end of swelling practically returns to the dashed curve of the purely mechanical cycle, see Fig. 6 in LHG (2002). The reason of this different behaviour is due to the presence of two cations in the solid phase of Bisaccia clay. The initial state contains the two cations in a certain proportion, point P₁ in Fig. 4(a). Increase of the Na-content leads to a decrease of κ , point P₂, but later chemical

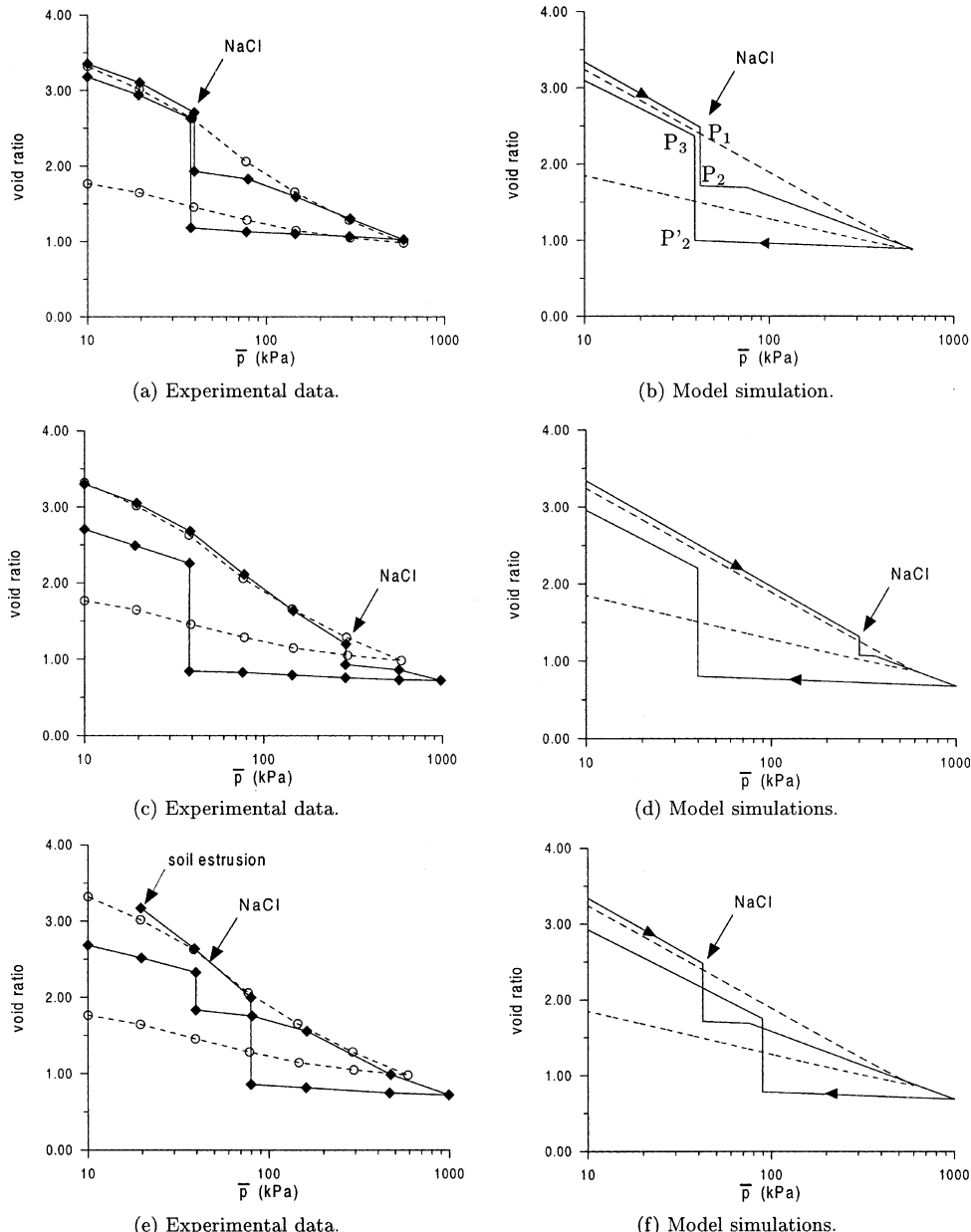


Fig. 3. Mechanical load cycle on Bisaccia clay exposed to distilled water (dashed curve). Chemo-mechanical loading cycles with replacement of the distilled water solution by a NaCl-saturated solution, later replaced itself by the distilled water solution (solid curve). The three sets of data and simulations differ by the mean-stresses at which chemical loading and unloading are performed. Replacement of preexisting cations K^+ in the clay cluster by cations Na^+ implies that swelling is larger than chemical consolidation as explained by the increase of mechanical compliances shown in Fig. 4(a). Experimental data by Di Maio and Fenelli (1997), their Fig. 7.

unloading leads to a value of κ larger than the initial one, point P_3 , Fig. 4(a). Mechanical loading-unloading has a small effect on the chemical composition of the solid phase, so that the state does not change significantly from the end of the chemical consolidation to the beginning of chemical swelling, i.e. $P_2 \approx P'_2$.

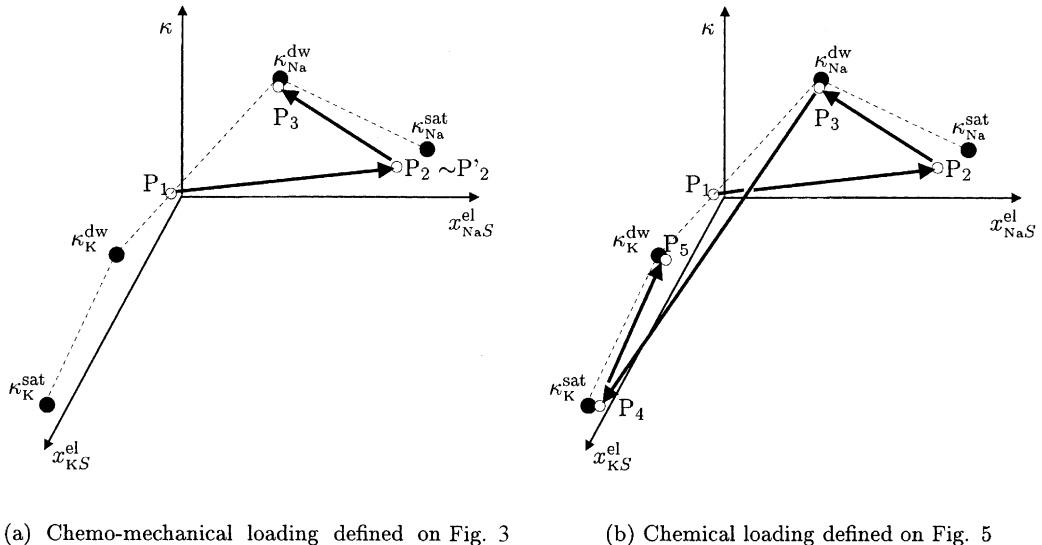


Fig. 4. Qualitative evolution of the elastic compliance κ during the chemical loadings described by Figs. 3 and 5. The initial state, Point P_1 , is located on the line of minimal cation content which ensures electroneutrality for a distilled pore water, see Fig. 2. The subsequent changes of the chemical content of pore water leads to changes in the solid phase which are accompanied with variations of κ , Points P_2 to P_5 , as described in Appendix A. As a general rule, both compliances κ and λ are much smaller on the K-plane than on the Na-plane.

The fact that κ is larger at P_3 than at P_1 is responsible for the larger swelling observed in the simulations of Fig. 3, in agreement with experimental data. On the other hand, for the Ponza bentonite studied in LHG (2002), the whole process was occurring in the Na-plane of Fig. 4(a), so that the initial and final values of κ , like their representative points P_1 and P_3 , were quite close.

Due to irreversibilities and non-linearities involved in chemical coupling, model simulations of chemical loading and unloading will be highly dependent on the assigned path in terms of the mass contents or molar fractions of the species in pore water. In the following, for the sake of simplicity, we assume that the sample is in contact with a water reservoir having a volume equal to the pore volume of the sample. Actually the volume of water surrounding a sample in an oedometric cell is usually larger than the value here assumed. The chemical loading is simulated by adding a controlled mass of NaCl salt to free and pore water. This addition induces an increase of the molar fraction x_{NaW} , which, in the initial phase of loading, is counterbalanced by the release of K^+ from absorbed water, point P_1 to point P_2 in Fig. 5(b). This counterbalance phenomenon is particularly important at low values of x_{NaW} and induces the curved increase of the relative weight of Na^+ in the solid phase as shown in Fig. 6 from point P_1 to point P_2 . In fact, one should stress that the exact experimental set up has a quantitative influence on the absorption/desorption processes. For example, increasing the ratio volume of reservoir water versus volume of pore water decreases the curvature of the path P_1 to P_2 . The chemical unloading was simulated by the subtraction of masses of both NaCl and KCl from the reservoir and pore water, point P_2 to point P_3 in Figs. 5(b), 6: the idea is to mimic the frequent substitutions of reservoir water performed experimentally.

5.3. Chemical loading cycles involving two salts

After equilibrium with a distilled pore water at $\bar{p} = 40$ kPa has been reached, cycles of chemical loading and unloading are applied while the effective stress is kept fixed. A chemical cycle consists in exposing the sample to a salt-saturated solution (chemical loading), subsequently replaced by distilled water (chemical unloading). The salts used here are NaCl and KCl. Results are presented in Figs. 5–8.

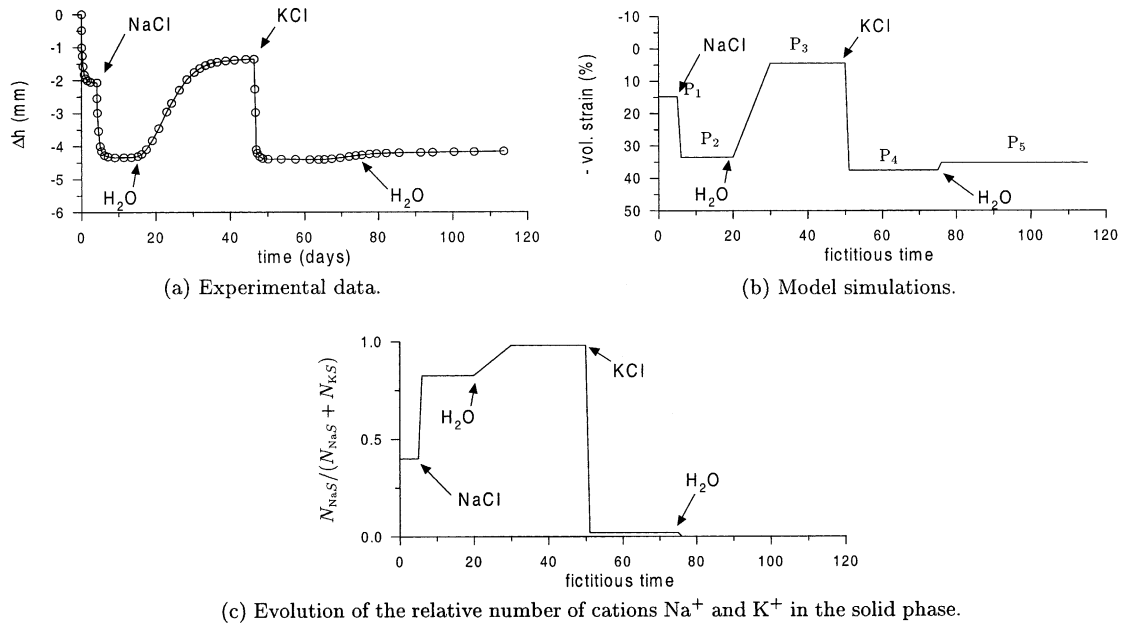


Fig. 5. Complex chemical loading on Bisaccia clay with successive replacements of the pore solution after equilibrium has been reached under the fixed effective mean-stress $\bar{\sigma} = 40$ kPa. Pore solution is 1/ distilled water, 2/ a Na-saturated solution, 3/ distilled water, 4/ a K-saturated solution, and finally 5/ distilled water. Replacement of preexisting cations K^+ by cations Na^+ implies that the first swelling is larger than chemical consolidation, and the second swelling much smaller in agreement with Fig. 2. Evolution during the process of (a) the height of the oedometer, (b) the volumetric strain, (c) the relative number of cations Na^+ in the solid phase. Experimental data by Di Maio and Fenelli (1997), their Fig. 4.

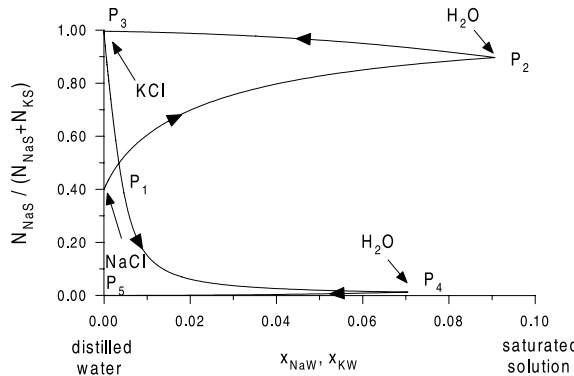


Fig. 6. Evolution of the relative number of cations Na^+ in the solid phase with respect to the total number of exchangeable cations N_{ex} for the loading process on Bisaccia clay of Fig. 5.

Tests concern Bisaccia clay, Fig. 5, and Ponza bentonite, Fig. 8. For Bisaccia clay, the first chemical consolidation due to saturation of pore water by NaCl leads to some plasticity as described in relation to Fig. 3. Also in agreement with the observations regarding that figure, the amount of contractancy due to plasticity is not sufficient to overcome the increase of κ due to the subsequent exposure to distilled water, path P₂ to P₃ in Fig. 4(b): therefore the chemical cycle results in a net dilatancy. However for Ponza clay, the initial state is much closer to the Na-plane in Fig. 2. Therefore, the change of κ at the end of the

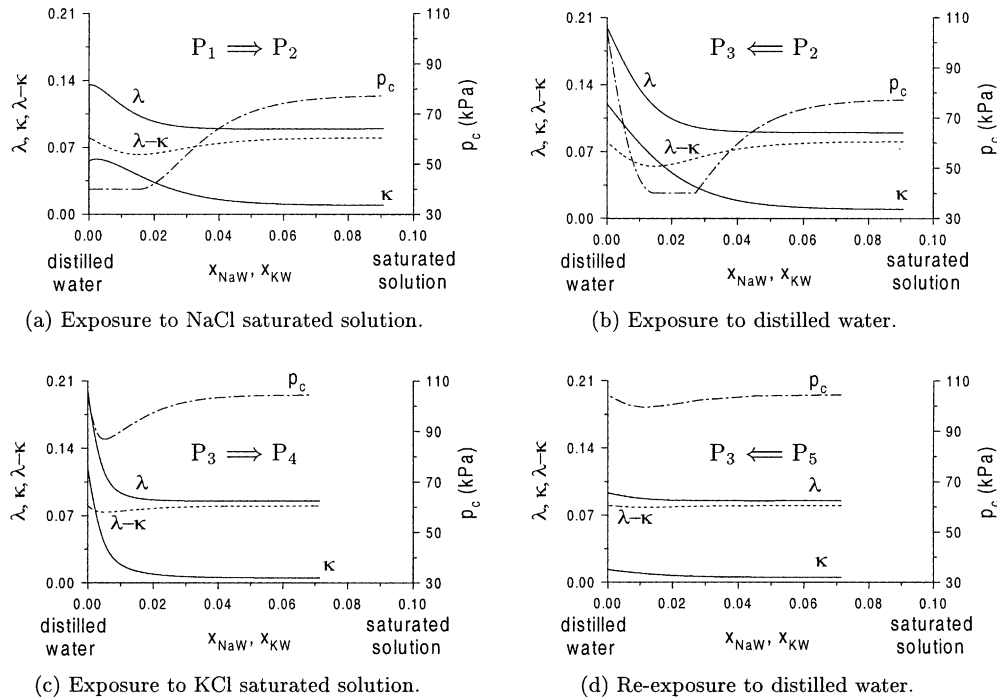


Fig. 7. Evolution of the mechanical properties and of the preconsolidation stress p_c during chemical loadings and unloadings at constant $\bar{p} = 40$ kPa shown in Fig. 5. The behaviour is elastic-plastic initially: plastic contractancy occurs first to compensate for chemical softening and maintain constant $p_c = \bar{p}$. Where the chemical influence on p_c is positive, it results in an elastic behaviour and preconsolidation. The subsequent exposure to water (b) shows also some plasticity (where p_c is equal to the applied \bar{p}) which disappears in the next cycle, (c), (d). The successive points P_1, \dots, P_5 refer to Fig. 6.

chemical cycle is quite small, and consequently, the occurrence of plasticity during chemical consolidation results in a net contractancy at the end of the first cycle.

The first exposure to a KCl saturated pore water solution leads to a large decrease of κ , path P_3 to P_4 in Fig. 4(b): since $\kappa_K^{\text{sat}} - \kappa_{\text{Na}}^{\text{dw}} = -0.115$ is almost equal to $\kappa_{\text{Na}}^{\text{sat}} - \kappa_{\text{Na}}^{\text{dw}} = -0.110$, the associated decrease of volume is quite similar (to within the sign) to the volume increase due to the previous exposure to distilled pore water, Figs. 5 and 8. Subsequent exposures to distilled water and KCl saturated solutions display small volume changes since the values of κ remain small as the path remains close to the K-plane in Fig. 4(b), e.g. path P_4 to P_5 associated to Fig. 5.

The effect of the equilibrium constant K_{eq} , also referred to as selectivity coefficient, is illustrated by the evolution of the relative number of cations Na^+ with respect to the total number of cations present in the solid phase, Figs. 5(c) and 8(c). In fact, saturation of the pore water by NaCl leads to a relative increase of cations Na^+ in the solid phase, but the percentage of cations K^+ that are not desorbed is still significant at the end of the first cycle. On the other hand, saturation of the pore water by KCl leads to almost complete desorption of the cations Na^+ . This information is also readable from Fig. 6 which provides in addition the quantitative evolution of the relative number of cations Na^+ with the chemical content of pore water.

Notice that the model forecasts a progressive replacement of the absorbed cations by cations Na^+ at the first stage of loading history, Fig. 8(c). However, the amplitude of the phenomenon is much smaller than experimentally observed, Fig. 8(a). One explanation might be that the initial content in absorbed cations Na^+ is smaller than assumed in the simulations.

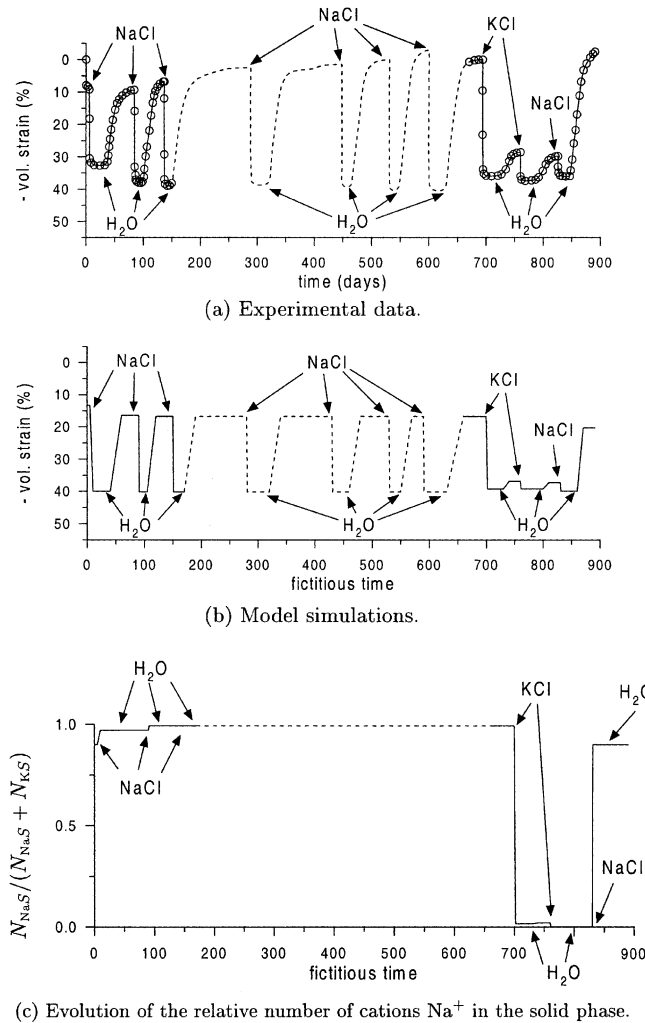


Fig. 8. After equilibrium has been reached under the fixed effective mean-stress $\bar{p} = 40$ kPa, a complex chemical loading is performed consisting of successive replacements of the pore solution. Experimental data on Ponza bentonite by Di Maio (1998), her Fig. 15. The presence of cations K^+ stiffens significantly the mechanical properties.

Since we are concerned here with pointwise material properties, the time scale along the abscissa in Figs. 5 and 8(b), (c) is purely fictitious: only the equilibrium values (horizontal segments) are obtained by the constitutive equations. In order to obtain the time-evolution of the volume change of the sample, a complete initial and boundary value problem involving transfer and diffusion effects will have to be considered (Gajo and Loret, 2002).

6. Comparison with the model of LHG (2002) and conclusions

The model developed here can be viewed as extending the classic elastic–plastic framework for porous media to account for electro-chemo-mechanical couplings. Therefore, it can capitalize upon the available

theoretical and computational developments in view of solving initial and boundary value problems in a multi-dimensional setting. Although analyses of instrumented in situ cases are the ultimate goal, it will be necessary in a first step to simulate laboratory tests to check the validity of certain assumptions that have been made to interpret the experimental results, e.g. assumption of chemical equilibrium and homogeneity of the chemical fields throughout the sample at the times where measurements are made. Such an analysis is presented in Gajo and Loret (2002).

The present electro-chemo-mechanical constitutive model for heteroionic clays (used for two cations) reduces smoothly to the chemo-mechanical model for Na-Montmorillonite clays when the relative fraction of cations Na^+ overweights that of K^+ . In fact, the present simulations of Ponza clay displays two modifications with respect to the ones shown in LHG (2002). In LHG (2002), salt was not allowed to transfer from the solid phase to the fluid phase and conversely, although the general scheme allowed for that possibility. The reason to prevent that transfer was that the model did not recognize cations and anions but only salts, e.g. NaCl , and so transfer of Na^+ in the solid phase would have brought anions Cl^- as well. On the other hand as in LHG (2002), the *total* amount of absorbed salts, that is cations and anions, is constant, due to the assumption of a negligible amount of chloride anions and electroneutrality. A second modification is that the present model recognizes that Ponza bentonite, although an essentially Na-Montmorillonite, contains also cations K^+ whose relative weight strongly matters. Therefore while the representative states of the solid phase shown in Figs. 2 and 4 were *in* the Na-plane in LHG (2002), they are now, more realistically, *close* to that plane as long as pore water is distilled or contains NaCl . If another cation, like K^+ , of selectivity constant greater than one with respect to Na^+ is dissolved in pore water, it transfers at a fast rate in the solid phase, e.g. Figs. 6 and 8(c), the cations Na^+ are desorbed and the representative states in Fig. 4 leaves the Na-plane to get closer to the K-plane.

The model is three-dimensional, even if the first basic verifications presented here concern isotropic loadings. Drained and undrained triaxial tests, for which experimental data exist, have been simulated in LHG (2002).

The data available show that cations Na^+ and, more drastically, K^+ stiffen significantly the mechanical properties κ and λ . Data from Di Maio and Onorati (1999) also show that samples in contact with a NaCl solution have a friction angle which increases with the salt content of the solution. The model presented here can incorporate the variation of friction angle due to chemical content of the solid phase through the parameter M , Appendix C. However, we do not have available data showing whether or not exposure of samples to KCl solutions has a still stronger effect on the friction angle than exposure to NaCl solutions. For that purpose, triaxial drained or undrained tests have to be performed.

Acknowledgements

The authors thank C. Di Maio for providing them with several unpublished experimental data. AG acknowledges a visiting fellowship at Ecole Nationale Supérieure d'Hydraulique et Mécanique de Grenoble and TH a senior fellowship from the french Ministère de l'Enseignement Supérieur et de la Recherche.

Appendix A. Chemical interpolation of the elastic coefficient κ

To estimate the effect of pore water composition on the elastic coefficient κ , one has in a first step to find the elastic molar fractions x_{ks}^{el} , $k \in S^{\leftrightarrow}$, which initially are equal to the total molar fractions x_{ks} : these quantities are not controlled, they are a by-product of the constitutive equations.

With this preliminary step in mind, we consider in turn the two hypothetical extreme situations where the molar fraction of one cation, say cation Na^+ , overweights the other in both phases. We get measures or approximations of the values of $\kappa_{\text{Na}}^{\text{dw}}$ and $\kappa_{\text{Na}}^{\text{sat}}$ corresponding respectively to a distilled and salt-saturated

pore water. Then, chemical influence of absorbed water on κ is introduced through interpolation between these two situations. The same calibration is performed on the K-plane where the molar fraction of cations K^+ overweights that of cations Na^+ .

The complete expression of κ is obtained by a second interpolation over the molar fractions of the cations.

The notations $(x_{IS}^{\text{el}})^{k\text{sat}}$ and $(x_{IS}^{\text{el}})^{k\text{dw}}$ refer to the molar fractions where only cation k is present in the solid phase and the pore water solution is either k -saturated or distilled water. The influence of absorbed water is introduced via the scaling functions $\theta_k(x_{ws}^{\text{el}})$,

$$\theta_k(x_{ws}^{\text{el}}) = \frac{x_{ws}^{\text{el}} / (x_{ws}^{\text{el}})^{k\text{dw}} - 1}{(x_{ws}^{\text{el}})^{k\text{sat}} / (x_{ws}^{\text{el}})^{k\text{dw}} - 1}, \quad k = Na, K, \quad (A.1)$$

and the individual influence of the cations by the weighting function ω_k ,

$$\omega_k(x_{NaS}^{\text{el}}, x_{KS}^{\text{el}}) = \frac{x_{kS}^{\text{el}}}{x_{NaS}^{\text{el}} + x_{KS}^{\text{el}}}, \quad k = Na, K, \quad (A.2)$$

and so $\omega_{Na} = 1 - \omega_K$. The elastic coefficient κ_k on the plane k is assumed in the form

$$\kappa_k = \kappa_k(x_{ws}^{\text{el}}) = \kappa_{1k}\Phi(\kappa_{3k}\theta_k) + \kappa_{2k}, \quad k = Na, K. \quad (A.3)$$

For definiteness, we take

$$\Phi(0) = 0, \quad \Phi'(0) \equiv \frac{d\Phi}{dy}(y=0) = 1. \quad (A.4)$$

For example, Φ may be the hyperbolic tangent $tanh$ and then $\Phi'(y) = 1 - \tanh^2(y)$.

The coefficients κ_{1k} , κ_{2k} and κ_{3k} are obtained from the four measurable quantities $\kappa^{k\text{dw}}$ and $\kappa^{k\text{sat}}$ and from the slopes $d\kappa/dx_{ws}^{\text{el}} = (x_{ws}^{\text{el}})^{k\text{dw}}$, $k = Na, K$, namely

$$\kappa_{2k} = \kappa_k^{\text{dw}}, \quad \kappa_{1k} = \frac{\kappa_k^{\text{sat}} - \kappa_k^{\text{dw}}}{\Phi(\kappa_{3k})}, \quad k = Na, K, \quad (A.5)$$

and

$$\frac{\kappa_{3k}}{\Phi(\kappa_{3k})} = \frac{(x_{ws}^{\text{el}})^{k\text{sat}} - (x_{ws}^{\text{el}})^{k\text{dw}}}{\kappa_k^{\text{sat}} - \kappa_k^{\text{dw}}} \frac{d\kappa}{dx_{ws}^{\text{el}}} (x_{ws}^{\text{el}} = (x_{ws}^{\text{el}})^{k\text{dw}}), \quad k = Na, K. \quad (A.6)$$

Next, one defines an interpolation between the Na- and K-planes,

$$\kappa = \kappa_1\Phi(\kappa_3\theta) + \kappa_2, \quad (A.7)$$

with

$$\kappa_1 = \sum_{k=Na, K} \omega_k \kappa_{1k}, \quad \kappa_2 = \sum_{k=Na, K} \omega_k \kappa_{2k}, \quad \kappa_3 \theta(x_{ws}^{\text{el}}) = \sum_{k=Na, K} \omega_k \kappa_{3k} \theta_k(x_{ws}^{\text{el}}). \quad (A.8)$$

The following derivatives are needed,

$$\frac{\partial \omega_k}{\partial x_{kS}^{\text{el}}} = -\frac{\partial \omega_l}{\partial x_{kS}^{\text{el}}} = \frac{\omega_k}{x_{kS}^{\text{el}}} (I_{kl} - \omega_l), \quad k, l = Na, K, \quad (A.9)$$

and

$$\frac{d\theta_k}{dx_{ws}^{\text{el}}} = \frac{1}{(x_{ws}^{\text{el}})^{k\text{sat}} - (x_{ws}^{\text{el}})^{k\text{dw}}}, \quad k = Na, K, \quad (A.10)$$

in order to calculate

$$d\kappa = \sum_{k=\text{Na, K}} (\kappa_{1k}\Phi(\kappa_3\theta) + \kappa_{2k} + \kappa_1\kappa_{3k}\theta_k\Phi'(\kappa_3\theta))d\omega_k + \kappa_1\kappa_{3k}\omega_k\Phi'(\kappa_3\theta)d\theta_k. \quad (\text{A.11})$$

which in turn, together with (2.18), is used to calculate

$$\frac{\partial\kappa}{\partial m_{kS}^{\text{el}}} = \sum_{l \in S^+ \cup \{w\}} \frac{\partial\kappa}{\partial x_{lS}^{\text{el}}} \frac{\partial x_{lS}^{\text{el}}}{\partial m_{kS}^{\text{el}}}. \quad (\text{A.12})$$

Simplifications arise if the relation (3.31) is used. Indeed, then $\omega_k = N_{kS}^{\text{el}}/N_{\text{ex}}$, so that $d\omega_k/dm_{kS}^{\text{el}} = V_0/N_{\text{ex}}m_k^{(\text{M})}$ and

$$d\kappa = \frac{\partial\kappa}{\partial m_{\text{NaS}}^{\text{el}}} dm_{\text{NaS}}^{\text{el}} + \frac{\partial\kappa}{\partial m_{\text{wS}}^{\text{el}}} dm_{\text{wS}}^{\text{el}}, \quad (\text{A.13})$$

with

$$\frac{\partial\kappa}{\partial m_{\text{NaS}}^{\text{el}}} = \frac{V_0}{N_{\text{ex}}m_{\text{Na}}^{(\text{M})}} ((\kappa_{1\text{Na}} - \kappa_{1\text{K}})\Phi(\kappa_3\theta) + (\kappa_{2\text{Na}} - \kappa_{2\text{K}}) + (\kappa_{3\text{Na}}\theta_{\text{Na}} - \kappa_{3\text{K}}\theta_{\text{K}})\kappa_1\Phi'(\kappa_3\theta)), \quad (\text{A.14})$$

and

$$\frac{\partial\kappa}{\partial m_{\text{wS}}^{\text{el}}} = \kappa_1\Phi'(\kappa_3\theta) \frac{\partial x_{\text{wS}}^{\text{el}}}{\partial m_{\text{wS}}^{\text{el}}} \sum_{k=\text{Na, K}} \kappa_{3k}\omega_k \frac{d\theta_k}{dx_{\text{wS}}^{\text{el}}}. \quad (\text{A.15})$$

Appendix B. Elastic–plastic stiffness

The coefficients $f_k, g_k, k \in \{p, q, S^\leftarrow\}$ entering the elastic–plastic stiffness (4.11) are obtained by writing the consistency condition $\delta f = 0$:

$$\begin{cases} f_k = -B_{kp} \frac{\partial f}{\partial \bar{p}} + \sum_{l \in S^+ \cup \{w\}} \beta_{kl} \frac{\partial f}{\partial \bar{\mu}_{lS}}, & k \neq q, \quad f_q = 3G \frac{\partial f}{\partial q} \\ g_k = -B_{kp} \frac{\partial g}{\partial \bar{p}} + \sum_{l \in S^+ \cup \{w\}} \beta_{kl} \frac{\partial g}{\partial \bar{\mu}_{lS}}, & k \neq q, \quad g_q = 3G \frac{\partial g}{\partial q}. \end{cases} \quad (\text{B.1})$$

The plastic modulus H is assumed to take only strictly positive values,

$$H = h + B_{pp} \frac{\partial f}{\partial \bar{p}} \frac{\partial g}{\partial \bar{p}} + 3G \frac{\partial f}{\partial q} \frac{\partial g}{\partial q} - \sum_{k \in S^+ \cup \{w\}} B_{kp} \left(\frac{\partial f}{\partial \bar{p}} \frac{\partial g}{\partial \bar{\mu}_{kS}} + \frac{\partial g}{\partial \bar{p}} \frac{\partial f}{\partial \bar{\mu}_{kS}} \right) + \sum_{k, l \in S^+ \cup \{w\}} \beta_{kl} \frac{\partial f}{\partial \bar{\mu}_{kS}} \frac{\partial g}{\partial \bar{\mu}_{lS}}, \quad (\text{B.2})$$

while the hardening modulus h will be positive for hardening, and negative for softening,

$$h = \frac{p_c}{\lambda - \kappa} \frac{\partial g}{\partial \bar{p}}. \quad (\text{B.3})$$

For the Modified Cam–Clay model (4.14), the following derivatives are needed,

$$\frac{\partial f}{\partial \bar{p}} = 1 - \frac{1}{M^2} \frac{q^2}{\bar{p}^2}, \quad \frac{\partial f}{\partial q} = \frac{2}{M^2} \frac{q}{\bar{p}}, \quad \frac{\partial f}{\partial \bar{\mu}_{kS}} = -\frac{2}{M^3} \frac{q^2}{\bar{p}} \frac{\partial M}{\partial \bar{\mu}_{kS}} - \frac{\partial p_c}{\partial \bar{\mu}_{kS}}, \quad k \in S^+ \cup \{w\}. \quad (\text{B.4})$$

where

$$\frac{\partial p_c}{\partial \bar{\mu}_{KS}} = \left(\ln \frac{\bar{p}_\lambda}{p_c} \frac{\partial \lambda}{\partial \bar{\mu}_{KS}} - \ln \frac{\bar{p}_\kappa}{p_c} \frac{\partial \kappa}{\partial \bar{\mu}_{KS}} \right) \frac{p_c}{\lambda - \kappa} \quad (\text{B.5})$$

Appendix C. Chemical interpolations for the plastic coefficients λ and M in terms of $\{\bar{\mu}_{wS}, \bar{g}_{NaS} - \bar{g}_{KS}\}$

To estimate the effect of pore water composition on the plastic coefficients λ and M , one has in a first step to find the chemical potential of water and the chemical activity of cations in the solid phase. At equilibrium, these quantities are simply equal to their counterparts in the fluid phase. Since the chemical effects on these two coefficients are assumed to be similar, we just consider one of them, say $\lambda = \lambda(\bar{\mu}_{wS}, \bar{g}_{NaS} - \bar{g}_{KS})$.

We consider in turn the two hypothetical extreme situations where the molar fraction of one cation, say cation Na^+ , overweights the other in both phases. We may get measures or approximations of the values of $\lambda_{\text{Na}}^{\text{dw}}$ and $\lambda_{\text{Na}}^{\text{sat}}$ corresponding respectively to a distilled and salt-saturated pore water. Then the chemical effect on λ , noted λ_{Na} , is introduced through interpolation between these two situations, for example

$$\lambda_{\text{Na}}(\bar{\mu}_{wS}) = \lambda_{1\text{Na}} \Phi(\lambda_{3\text{Na}} \theta_{\text{Na}}(\bar{\mu}_{wS})) + \lambda_{2\text{Na}}, \quad (\text{C.1})$$

where the $\lambda_{i\text{Na}}$'s, $i = 1, 3$, are constants. The hyperbolic tangent is taken as the interpolation function, i.e. $\Phi(y) = \tanh(y)$ and

$$\theta_k(\bar{\mu}_{wS}) = \frac{\phi(\bar{\mu}_{wS}) - \phi(\bar{\mu}_{wS}^{\text{dw}})}{\phi(\bar{\mu}_{wS}^{\text{sat}}) - \phi(\bar{\mu}_{wS}^{\text{dw}})}, \quad (\text{C.2})$$

where

$$\phi(\bar{g}_{KS}) = \exp\left(\frac{\bar{g}_{KS}}{RT}\right), \quad k = \text{Na, K, w}. \quad (\text{C.3})$$

Then

$$\lambda_{1\text{Na}} = \frac{\lambda_{\text{Na}}^{\text{sat}} - \lambda_{\text{Na}}^{\text{dw}}}{\Phi(\lambda_{3\text{Na}})}, \quad \lambda_{2\text{Na}} = \lambda_{\text{Na}}^{\text{dw}}. \quad (\text{C.4})$$

The constant $\lambda_{3\text{Na}}$ can be obtained from the slope $d\lambda/d\bar{\mu}_{NaS}$ estimated at $\bar{\mu}_{wS} = \bar{\mu}_{wS}^{\text{dw}}$, indeed

$$\frac{\lambda_{3\text{Na}}}{\tanh(\lambda_{3\text{Na}})} = \frac{\phi(\bar{\mu}_{wS}^{\text{sat}}) - \phi(\bar{\mu}_{wS}^{\text{dw}})}{\lambda_{\text{Na}}^{\text{sat}} - \lambda_{\text{Na}}^{\text{dw}}} \frac{d\lambda_{\text{Na}}}{d\bar{\mu}_{wS}} \left(\frac{d\phi}{d\bar{\mu}_{wS}} \right)^{-1}. \quad (\text{C.5})$$

The same procedure is followed to define the $\lambda_{i\text{K}}$, $i = 1, 3$.

Next, one defines an interpolation between the Na- and K-planes,

$$\lambda = \lambda_1 \Phi(\lambda_3 \theta) + \lambda_2, \quad (\text{C.6})$$

with

$$\lambda_1 = \sum_{k=\text{Na, K}} \tilde{\omega}_k \lambda_{1k}, \quad \lambda_2 = \sum_{k=\text{Na, K}} \tilde{\omega}_k \lambda_{2k}, \quad \lambda_3 \theta(\bar{\mu}_{wS}) = \sum_{k=\text{Na, K}} \tilde{\omega}_k \lambda_{3k} \theta_k(\bar{\mu}_{wS}). \quad (\text{C.7})$$

The weights $\tilde{\omega}_{\text{Na}}$ and $\tilde{\omega}_{\text{K}}$, with sum equal to 1, are defined as follows,

$$\tilde{\omega}_k(\bar{g}_{NaS}, \bar{g}_{KS}) = \frac{\phi(\bar{g}_{KS})}{\phi(\bar{g}_{KS}) + \phi(\bar{g}_{IS})} = \frac{1}{1 + \phi(\bar{g}_{IS} - \bar{g}_{KS})}, \quad k \neq l = \text{Na, K}. \quad (\text{C.8})$$

The following derivatives

$$d\tilde{\omega}_{Na} = \frac{\tilde{\omega}_{Na}\tilde{\omega}_K}{RT} (d\bar{g}_{NaS} - d\bar{g}_{KS}), \quad d\theta_k = \frac{\phi(\bar{\mu}_{wS})}{\phi_k^{\text{sat}} - \phi_k^{\text{dw}}} \frac{d\bar{\mu}_{wS}}{RT}, \quad k = Na, K, \quad (C.9)$$

are needed in order to calculate

$$d\lambda = ((\lambda_{1Na} - \lambda_{1K})\Phi(\lambda_3\theta) + (\lambda_{2Na} - \lambda_{2K}) + (\lambda_{3Na}\theta_{Na} - \lambda_{3K}\theta_K)\lambda_1\Phi'(\lambda_3\theta))d\tilde{\omega}_{Na} + \left(\tilde{\omega}_{Na}\lambda_{3Na} \frac{d\theta_{Na}}{d\bar{\mu}_{wS}} + \tilde{\omega}_K\lambda_{3K} \frac{d\theta_K}{d\bar{\mu}_{wS}} \right) \lambda_1\Phi'(\lambda_3\theta)d\bar{\mu}_{wS}. \quad (C.10)$$

Appendix D. Determination of the initial state in the solid phase

We seek for an initial approximation of the state in the solid phase while the chemical composition of pore water corresponds to distilled water. The following data are assumed to be either known or guessed:

- void ratio e ;
- ratio N_{wW}/N_{wS} of the number of moles of water in the fluid and solid phases;
- ratio N_{KS}/N_{NaS} of the number of moles of cations in the solid phase;
- ratio N_{ClS}/N_{NaS} of the number of moles of Cl^- versus Na^+ assumed to be very small;
- α : volume percentage of absorbed water that evaporates only at very high temperature;
- valences of all species; for an anhydrous smectite of formula $NaAl_3Si_3O_{10}(OH)_2$, Ransom and Helgeson (1994) find approximately a volume average of three moles of clay for one mole of Na^+ , so $\zeta_c = -1/3$. The analysis below holds for arbitrary valences.
- molar volumes of water $v_{wS}^{(M)} = 18 \text{ cm}^3$, of Na^+ , $v_{NaS}^{(M)} = 2.66 \text{ cm}^3$, of K^+ , $v_{KS}^{(M)} = 5.93 \text{ cm}^3$, of clay particles, e.g. for the above smectite, Ransom and Helgeson (1994) have obtained, using the technique of structural analogy, $v_{cS}^{(M)} \sim 146 \text{ cm}^3$.

The physical properties (molar mass, molar volume, density) of the species are assumed to be identical in both phases, Eq. (2.9).

Using electroneutrality in the solid phase, the ratio of the number of moles of Na^+ versus clay can be expressed in terms of given quantities,

$$\frac{N_{NaS}}{N_{cS}} \left(\zeta_{Na} + \zeta_K \frac{N_{KS}}{N_{NaS}} + \zeta_{Cl} \frac{N_{ClS}}{N_{NaS}} \right) = -\zeta_c. \quad (D.1)$$

The initial void ratio is

$$e = \frac{V_{wW} + (1 - \alpha)V_{wS} + V_{NaW} + V_{Kw} + V_{Clw}}{V_{cS} + \alpha V_{wS} + V_{NaS} + V_{KS} + V_{ClS}}. \quad (D.2)$$

Since the pore water is distilled water, the molar fractions of ions in fluid phase are very small. Also the molar fractions of Cl^- is assumed to be negligible in the solid phase as well. The ratio of the number of moles of clay and absorbed water can be approximated in terms of now known quantities,

$$\frac{N_{cS}}{N_{wS}} \sim \frac{\frac{N_{wW}}{N_{wS}} + 1 - \alpha - \alpha e}{v_{cS}^{(M)} + \frac{N_{NaS}}{N_{cS}} \left(v_{NaS}^{(M)} + \frac{N_{KS}}{N_{NaS}} v_{KS}^{(M)} \right)} \frac{v_{wW}^{(M)}}{e}. \quad (D.3)$$

Using the definition (2.10) of x_{wS} and again electroneutrality in the solid phase, the molar fraction of absorbed water is obtained as

$$\frac{1}{x_{ws}} = 1 + \frac{N_{cs}}{N_{ws}} \left(1 - \frac{\zeta_c}{\zeta_{Na}} + \left(1 - \frac{\zeta_K}{\zeta_{Na}} \right) \frac{N_{KS}}{N_{NaS}} \frac{N_{NaS}}{N_{cs}} + \left(1 - \frac{\zeta_{Cl}}{\zeta_{Na}} \right) \frac{N_{ClS}}{N_{NaS}} \frac{N_{NaS}}{N_{cs}} \right), \quad (D.4)$$

from which the other molar fractions are deduced,

$$x_{cs} = \frac{N_{cs}}{N_{ws}} x_{ws}, \quad x_{NaS} = \frac{N_{NaS}}{N_{cs}} x_{cs}, \quad x_{KS} = \frac{N_{KS}}{N_{NaS}} x_{NaS}. \quad (D.5)$$

In a unit volume of porous medium, the number of moles of absorbed water is, using (D.4),

$$N_{ws} \sim \frac{e}{1+e} \frac{1}{1 + \frac{N_{ww}}{N_{ws}}} \frac{1}{\alpha v_{ww}^{(M)}}, \quad (D.6)$$

from which the volume and mass of absorbed water per unit volume of porous medium can be estimated, namely $v_{ws} = N_{ws} v_{ws}^M$ and $m_{ws} = N_{ws} m_w^{(M)}$. The volume and mass of free water are equal to their counterparts in the solid phase times N_{ww}/N_{ws} .

The number of moles of the other species is known from the above derivations. The following molar masses are needed to estimate the initial masses: $m_w^{(M)} = 18$ g, $m_{Na}^{(M)} = 23$ g, $m_K^{(M)} = 39.1$ g, $m_{Cl}^{(M)} = 35.5$ g and $m_c^{(M)} = 382$ g for the above anhydrous smectite which is used as an approximative reference for the simulations presented in this work.

Once the molar fractions in the solid phase are known, the data of the total molar fraction of ions $1 - x_{ww}$, the equilibrium constant (3.35), and the electroneutrality condition provide the individual molar fractions of ions in pore water,

$$x_{NaW} = \frac{1}{-\zeta_c} \frac{1 - x_{ww}}{1 + K_{eq} \frac{x_{KS}}{x_{NaS}}}, \quad x_{KW} = K_{eq} \frac{x_{KS}}{x_{NaS}} x_{NaW}, \quad x_{ClW} = x_{NaW} + x_{KW}. \quad (D.7)$$

Notice that, even if these molar fractions are very tiny, their ratio is not arbitrary.

As an alternative information to that provided by the void ratio, one might use the specific area, that provides the mass of absorbed water per unit mass of solid as the product of the size of the double layer, times the specific area, times the density of water.

The model uses interpolation between two extreme situations, one in which the fluid phase is distilled water and the other where it is salt saturated. Once the initial condition corresponding to distilled pore water has been obtained, the state of the solid phase in equilibrium with pore water saturated by a salt is obtained simply by solving the equations of equilibrium in terms of the chemical potentials of species that can transfer or, for the simplified model, in terms of the chemical potential of water and of the chemical activity.

References

Bataille, J., Kestin, J., 1977. Thermodynamics of mixtures. *J. Non-Equilib. Thermodyn.* 2, 49–65.

Bennethum, L.S., Cushman, J.H., 1999. Coupled solvent and heat transport of a mixture of swelling porous particles and fluids: single time-scale problem. *Transport Porous Med.* 36, 211–244.

Bolt, G.H., 1956. Physico-chemical analysis of the compressibility of pure clays. *Géotechnique* 6 (2), 86–93.

Charlez, Ph., Pradet, V., Pollard, R., Onaisi, A., Grégoire, M., 1998. How to manage wellbore stability in the Vicking Graben tertiary shales by using mud systems environmentally friendly? *Offshore Technology Conference*, Houston, 4–7 May 1998.

Di Maio, C., 1996. Exposure of bentonite to salt solution: osmotic and mechanical effects. *Géotechnique* 46 (4), 695–707.

Di Maio, C., 1998. Discussion on Exposure of bentonite to salt solution: osmotic and mechanical effects. *Géotechnique* 48 (3), 433–436.

Di Maio, C., Fenelli, G., 1997. Influenza delle interazioni chimico-fisiche sulla deformabilità di alcuni terreni argillosi. *Rivista Italiana di Geotecnica* 1, 695–707.

Di Maio, C., Onorati, R., 1999. Prove di laboratorio: influenza della composizione del liquido di cella. Rendiconti del XX Convegno Nazionale di Geotecnica, Parma, pp. 87–94.

Eringen, A.C., Ingram, J.D., 1965. A continuum theory for chemically reacting media-I. *Int. J. Eng. Sci.* 3, 197–212.

Gajo, A., Loret, B., 2002. Finite element simulations of electro-chemo-mechanical couplings in elastic–plastic heteroionic expansive clays, submitted for publication.

Haase, R., 1990. *Thermodynamics of Irreversible Processes*. Dover Publications, New York.

Heidug, W.K., Wong, S.-W., 1996. Hydration swelling of water-absorbing rocks: a constitutive model. *Int. J. Num. Anal. Meth. Geomech.* 20, 402–430.

Hueckel, T., 1992a. Water–mineral interaction in hygro-mechanics of clays exposed to environmental loads: a mixture approach. *Can. Geotech. J.* 29, 1071–1086.

Hueckel, T., 1992b. On effective stress concepts and deformation in clays subjected to environmental loads. *Can. Geotech. J.* 29, 1120–1125.

Huyghe, J.M., Janssen, J.D., 1999. Thermo-chemo-electro-mechanical formulation of saturated charged porous solids. *Transport Porous Med.* 34 (1–3), 129–141.

Kestin, J., 1968. *A Course in Thermodynamics*. Blaisdell Publishing Co., Waltham, Massachusetts.

Loret, B., Hueckel, T., Gajo, A., 2002. Chemo-mechanical coupling in saturated porous media: elastic–plastic behaviour of homoionic expansive clays. *Int. J. Solids Struct.* 39 (10), 2773–2806.

Ma, C.M., Hueckel, T., 1992. Effects of interphase mass transfer in heated clays: a mixture theory. *Int. J. Eng. Sci.* 30 (11), 1567–1582.

Murad, M.A., 1999. Thermo-mechanical model for hydration swelling in smectitic clays. *Int. J. Num. Anal. Meth. Geomech.*, Part I 27 (7), 673–696, Part II: 697–720.

Ransom, B., Helgeson, H.C., 1994. Estimation of the standard molal heat capacities, entropies and volumes of 2:1 clay minerals. *Geochim. Cosmochim. Acta* 58 (2), 4537–4547.

Sherwood, J.D., 1993. Biot poroelasticity of a chemically active shale. *Proc. R. Soc. Lond.* 440, 365–377.

Sherwood, J.D., 1994a. Swelling of shale around a cylindrical wellbore. *Proc. R. Soc. Lond.* 444, 161–184.

Sherwood, J.D., 1994b. A model of hindered solute transport in a poroelastic shale. *Proc. R. Soc. Lond.* 445, 679–692.

Tardy, Y., Duplay, J., 1992. A method of estimating the Gibbs free energies of formation of hydrated and dehydrated clay minerals. *Geochim. Cosmochim. Acta* 56, 3007–3029.